AFRL-AFOSR-UK-TR-2011-0059

Limitation of hot-carrier generated heat dissipation on the frequency of operation and reliability of novel nitride-based high-speed HFETs

Arvydas Matulionis

Semiconductor Physics Institute
A. Gostauto 11
Vilnius, Lithuania 2600

EOARD GRANT 09-3103

Report Date: 18 January 2012

Final Report for 15 July 2009 to 15 November 2011

Air Force Research Laboratory
Air Force Office of Scientific Research
European Office of Aerospace Research and Development
Unit 4515 Box 14, APO AE 09421

REPORT DOCUMENTATION PAGE

Form Approved OMB No. 0704-0188

1. REPORT DATE *(DD-MM-YYYY)*	2. REPORT TYPE	3. DATES COVERED *(From – To)*
18-01-2012	Final Report	15 Jul 2009 – 15 Nov 2011

4. TITLE AND SUBTITLE

Limitation of hot-carrier generated heat dissipation on the frequency of operation and reliability of novel nitride-based high-speed HFETs

5a. CONTRACT NUMBER

FA8655-09-1-3103

5b. GRANT NUMBER

Grant 09-3103

5c. PROGRAM ELEMENT NUMBER

61102F

6. AUTHOR(S)

Professor Arvydas Matulionis

5d. PROJECT NUMBER

5d. TASK NUMBER

5e. WORK UNIT NUMBER

7. PERFORMING ORGANIZATION NAME(S) AND ADDRESS(ES)

Semiconductor Physics Institute
A. Gostauto 11
Vilnius, Lithuania 2600

8. PERFORMING ORGANIZATION REPORT NUMBER

N/A

9. SPONSORING/MONITORING AGENCY NAME(S) AND ADDRESS(ES)

EOARD
Unit 4515 BOX 14
APO AE 09421

10. SPONSOR/MONITOR'S ACRONYM(S)

AFRL/AFOSR/RSW (EOARD)

11. SPONSOR/MONITOR'S REPORT NUMBER(S)

AFRL-AFOSR-UK-TR-2011-0059

12. DISTRIBUTION/AVAILABILITY STATEMENT

Approved for public release; distribution is unlimited.

13. SUPPLEMENTARY NOTES

14. ABSTRACT

The experimental investigation of fluctuations is a source of information on fast and ultrafast processes responsible for HFET performance and damage. A novel fluctuation-based approach, based on hot-electron velocity fluctuations measured at a microwave frequency, is used for prediction of nitride HFET operation and failure. The following statements summarize the main results: 1. The resonance-type dependence of hot-phonon lifetime on 2DEG density is resolved from the electron velocity fluctuations. 2. The optimal density for ultrafast dissipation of the LO-mode heat is estimated for the 2DEG channels located in GaN and InGaAs. 3. The optimal 2DEG density depends on the supplied power. 4. The HFET degradation is slower and the operation is faster when the LO-mode heat is dissipated faster. 5. The signatures of plasmons are found in electron velocity fluctuations, hot-phonon lifetime, electron drift velocity, HFET cutoff frequency, HFET phase noise, and HFET damage. 6. The novel heterostructre is proposed, implemented, and tested for improved ultrafast decay of LO-mode heat. 7. The novel heterostructre is proposed, implemented, and tested for improved efficiency of light emitting diodes. 8. The fluctuation-based approach is proposed for improved device performance and mitigated device damage.

15. SUBJECT TERMS

EOARD, solid state electronics, Electronic Materials

16. SECURITY CLASSIFICATION OF:			17. LIMITATION OF ABSTRACT	18, NUMBER OF PAGES	19a. NAME OF RESPONSIBLE PERSON
a. REPORT	b. ABSTRACT	c. THIS PAGE			SCOTT DUDLEY, Lt Col, USAF
UNCLAS	UNCLAS	UNCLAS	SAR	44	19b. TELEPHONE NUMBER *(Include area code)* +44 (0)1895 616162

Semiconductor Physics Institute
of
Center for Physical Science and Technology

AWARD NO. FA8655-09-1-3103
EUROPEAN OFFICE OF AEROSPACE RESEARCH AND DEVELOPMENT

Limitation of hot-carrier generated heat dissipation on the frequency of operation and reliability of novel nitride-based high-speed HFETs

Final Report
July 2009-November 2011
Vilnius 2011

List of Coauthors

H. Morkoç
Ü. Özgur
J. Xie,
J. H. Leach
V. Avrutin
M. Wu
X. Ni
J. Lee
X. Li
S. Liu
C. Y. Zhu
S. Okur
F. Zhang
C. Kayis
A. Ferreyra
J. Liberis
M. Ramonas
I. Matulionienė
E. Šermukšnis
L. Ardaravičius
O. Kiprijanovič
J. Kundrotas
A. Čerškus

Principal Investigator Arvydas Matulionis
Semiconductor Physics Institute of Center for Physical Science and Technology, Vilnius, Lithuania

Table of Contents

List of Tables

List of Figures

List of Publications

2009

1. A. Matulionis and H. Morkoc, "Hot phonons in InAlN/AlN/GaN heterostructure 2DEG channels (invited)", ***Proceedings of SPIE*** **7216**, 721608-1–14 (2009).
2. A. Matulionis, "GaN-based two-dimensional channels: hot-electron fluctuations and dissipation (invited)" ***Journal of Physics: Condensed Matter*** **21**(17) 174203-1–8 (2009).
3. J. Liberis, I. Matulionienė, A. Matulionis, E. Šermukšnis, J. Xie, J.H. Leach, and H. Morkoç, "InAlN-barrier HFETs with GaN and InGaN channels (invited)", ***Physica Status Solidi(A) Applications and Materials*** **206**(7) 1385–1395 (2009).
4. L. Ardaravičius, M. Ramonas, J. Liberis, O. Kiprijanovič, A. Matulionis, J. Xie, M. Wu, J.H. Leach, H. Morkoç, "Electron drift velocity in lattice matched AlInN/AlN/GaN channel at high electric field", ***Journal of Applied Physics*** **106**(7) 073708-1–5 (2009).
5. A. Matulionis, J. Liberis, I. Matulionienė, M. Ramonas, E. Šermukšnis, J. H. Leach, M. Wu, X. Ni, X. Li, H. Morkoç, "Plasmon-enhanced heat dissipation in GaN-based two-dimensional channels ", ***Applied Physics Letters*** **95**(19) 192102-1–3 (2009).
6. A. Matulionis, "Ultrafast decay of non-equilibrium (hot) phonons in GaN-based 2DEG channels(invited)", ***Physica Status Solidi (C)*** **6**(12) 2834–2839 (2009).
7. L. Ardaravičius, J. Liberis, O. Kiprijanovič, M. Ramonas, A. Matulionis, J. Xie, M. Wu, J.H. Leach, and H. Morkoç, "Strain dependent electron drift velocity in $Al_{1-x}In_xN$/AlN/GaN", ***Physica Status Solidi (C)*** **6**(12) 2635–2637 (2009).
8. J. H. Leach, M. Wu, X. Ni, J. Lee, Ü. Özgür, H. Morkoç, J. Liberis, E. Šermukšnis, A. Matulionis, H. Cheng, C. Kurdak, "Degradation in InAlN/GaN-based HFETs: Role of hot phonons" ***Applied Physics Letters*** **95**(22) 223504-1–3 (2009).
9. E. Šermukšnis, J. Liberis, and A. Matulionis, "Optimal 2DEG density for plasmon-assisted ultrafast decay of hot phonons", ***American Institute of Physics Conference Proceedings*** **1129** 245–248 (2009).
10. L. Ardaravičius, O. Kiprijanovič, J. Liberis, "Electric field strength and temperature dependence of conduction relaxation in AlGaN/AlN/GaN 2D electron gas" ***Lithuanian Journal of Physics*** **49**(4) 445–451 (2009)
11. A. Matulionis, J. Liberis, I. Matulionienė, M. Ramonas, E. Šermukšnis, J. H. Leach, M. Wu, X. Ni, X. Li, H. Morkoç, "Plasmon-enhanced heat dissipation in GaN-based two-dimensional channels" ***Virtual Journal of Ultrafast Science*** **8**(12) 1–3 (2009).

2010

12. A. Matulionis, J. Liberis, I. Matulionienė, M. Ramonas, E. Šermukšnis, „Ultrafast removal of LO-mode heat from a GaN-based two-dimensional channel" (invited), Special issue on GaN and ZnO Materials and Devices,Ed. H.Morkoç. ***Proceedings of*** **IEEE 98**(7) 1118–1126 (2010).
13. X. Ni, X. Li, J. Lee, S. Liu, V. Avrutin, Ü. Özgür, H. Morkoç, A. Matulionis, T. Paskova, G. Mulholland, and K.R. Evans, „InGaN staircase electron injector for reduced electron overflow in InGaN light emitting diodes," ***Applied Physics Letters*** **97**(3) 031110-1–3 (2010).

14. A. Matulionis, J. Liberis, H. Morkoç, "Plasmon-assisted dissipation of LO-mode heat in nitride 2DEG channels", ***Proceedings of SPIE* 7602**, 76020H-1-6 (2010).

15. J. H. Leach, X. Ni, J. Lee, Ü. Özgür, A. Matulionis, H. Morkoç, „New twists in LEDs and HFETs based on nitride semiconductors (invited)"**,** ***Physica Status Solidi (A) Applications and Materials*** **207**(5) 1091–1100 (2010).

16. J. H. Leach, M. Wu, X. Ni, X. Li, Ü. Özgür, H. Morkoç, J. Liberis, E. Šermukšnis, A. Matulionis, H. Cheng, Ç. Kurdak, Y.-T. Moon, "Stress test measurements of lattice matched InAlN/AlN/GaN HFET structures", ***Physica Status Solidi (A) Applications and Materials*** **207**(6) 1345–1347 (2010).

17. J. H. Leach, C. Y. Zhu, M. Wu, X. Ni, X. Li, J. Xie, Ü. Özgür, H. Morkoç, J. Liberis, E. Šermukšnis, A. Matulionis, T. Paskova, E. Preble, K. R. Evans, "Effect of hot phonon lifetime on electron velocity in InAlN/AlN/GaN heterostructure field effect transistors on bulk GaN substrates," ***Applied Physics Letters*** **96**(13) 133505/1–3 (2010).

18. X. Ni, X. Li, J. Lee, S. Liu, V. Avrutin, Ü. Özgür, H. Morkoç, A. Matulionis, T. Paskova, G. Mulholland, and K.R. Evans, "The effect of ballistic and quasi-ballistic electrons on the efficiency droop of InGaN light emitting diodes," ***Physica Status Solidi Rapid Research Letters*** **4**(8–9) 194–196 (2010).

19. A. Matulionis, J. Liberis, I. Matulionienė, E. Šermukšnis, J.H. Leach, H. Morkoç, „Optimal conditions for heat dissipation in nitride HFETs: Power tunable plasmon–LO-phonon resonance (invited), ***Proceedings of WOCSDICE*** **34** 191–194 (2010).

20. X. Ni, X. Li, J. Lee, S. Liu, V. Avrutin, Ü. Özgür, H. Morkoç, A. Matulionis, "Hot electron effects on efficiency degradation in InGaN light emitting diodes and designs to mitigate them," ***Journal of Applied Physics*** **108**(3) 033112-1–13 (2010).

21. X. Ni, X. Li, J. Lee, S. Liu, V. Avrutin, A. Matulionis, Ü. Özgür, and H. Morkoç, "Pivotal role of ballistic and quasi-ballistic electrons on LED efficiency (review)", ***Superlattices and Microstructures*** **48**(2) 133–153 (2010).

22. E. Šermukšnis, J. Liberis, and A. Matulionis, "Tuning into plasmon–LO-phonon resonance: gateless two-dimensional channels for nitride HEMTs", ***American Institute of Physics Conference Proceedings*** (Melville, New York) **1288** 109–112 (2010).

2011

23. A.Matulionis, J. Liberis, I. Matulionienė, E. Šermukšnis, J.H. Leach, M. Wu, H. Morkoç, "Novel fluctuation-based approach to optimization frequency performance and degradation of nitride heterostructure field effect transistors" (invited), ***Physica Status Solidi(A) Applications and Materials*** **208** (1) 30-36 (2011).

24. Ü. Özgür, X. Ni, X. Li, J. Lee, S. Liu, S. Okur, V. Avrutin, A. Matulionis**,** and H. Morkoç, "Ballistic transport in InGaN-based LEDs: impact on efficiency (invited)", ***Semiconductor Science and Technology*** **269(1)** 014022/1-12 (2011).

25. L. Ardaravičius, J. Liberis, O. Kiprijanovič, A. Matulionis, M. Wu, and H. Morkoç. "Hot-electron drift velocity and hot-phonon decay in AlInN/AlN/GaN" ***Physica Status Solidi Rapid Research Letters*** **5**(2–3) 65–67 (2011).

26. A.Matulionis, J. Liberis, I. Matulionienė, E. Šermukšnis, J. H. Leach, M. Wu, X. Ni, H. Morkoç, "Signature of hot phonons in reliability of nitride HFETs and signal delay" ***Acta Physica Polonica*** **A**. **119**(2) 225-227 (2011)

27. L. Ardaravičius¤, O. Kiprijanovič, and J. Liberis, "Hot-Phonon Decided Carrier Velocity in AlInN/GaN Based Two-Dimensional Channels" ***Acta Physica Polonica*** **A 119**(2) 231-233 (2011)

28. J. Kundrotas, A. Čerškus, J. Liberis, A. Matulionis, J.H. Leach, H. Morkoç, "Enhancement and narrowing of excitonic lines in AlInN/GaN heterostructures", ***Acta Physica Polonica*** **A. 119**(2) 173-175 (2011)

29. J. H. Leach, M. Wu, H. Morkoç, M. Ramonas, and A. Matulionis. „Heterostructure designs for enhanced performance and reliability in GaN HFETs: Camelback channels" ***Proceedings of SPIE*** **7939**, 79391P-1-10 (2011).

30. F. Zhang, X. Li, S. Liu, S. Okur, V. Avrutin, Ü. Özgür, and H. Morkoç, A. Matulionis, M. Kisin, „Impact of ballistic electron transport on efficiency of InGaN based LEDs", ***Proceedings of SPIE*** **7939** 793917-1-6 (2011).

31. A. Matulionis, M. Ramonas, E. Šermukšnis, J. Liberis, J.H. Leach, M. Wu, and H. Morkoç, „Mitigation of hot-phonon effects in a twin-channel nitride heterostructure field effect transistor", ***Proceedings of WOCSDICE*** **35** 82–83 (2011).

32. E. Šermukšnis, J. Liberis, M. Ramonas A. Matulionis, J.H. Leach, M. Wu, V. Avrutin, and H. Morkoç „Camelback channel for fast decay of LO phonons in GaN heterostructure field-effect transistor at high electron density", ***Applied Physics Letters*** **99** 043501 (2011)

33. C. Kayis, R. A. Ferreyra, M. Wu, X. Li, Ü. Özgür, A. Matulionis, H. Morkoç. „Degradation in InAlN/AlN/GaN heterostructure field-effect transistors as monitored by low-frequency noise measurements: Hot phonon effects", ***Applied Physics Letters*** **99** 063505 (2011)

34. E. Šermukšnis, J. Liberis, M. Ramonas A. Matulionis, J.H. Leach, M. Wu, V. Avrutin, and H. Morkoç „Camelback channel for fast decay of LO phonons in GaN heterostructure field-effect transistor at high electron density", ***Virtual Journal of Ultrafast Science*** **10**(8) 1–3 (2011).

35. X. Li, F. Zhang, S. Okur, V. Avrutin, S. J. Liu, Ü. Özgür, H. Morkoç, S. M. Hong, S. H. Yen, T. S. Hsu, and A. Matulionis, „On the quantum efficiency of InGaN light emitting diodes: Effects of active layer design, electron cooler, and electron blocking layer", ***Physica Status Solidi(A) Applications and Materials*** **208** (on line August 10, 2011).

Submitted Paper

36. J. H. Leach, M. Wu, H. Morkoç, J. Liberis, E. Šermukšnis, M. Ramonas, A. Matulionis, "Ultrafast decay of hot phonons in an AlGaN/AlN/AlGaN/GaN camelback channel", ***Journal of Applied Physics,*** accepted.

Reports at Conferences

37. A. Matulionis, H. Morkoç, Hot phonons in InN-contained heterostructure 2DEG channels (invited), ***SPIE Photonics West,*** *OPTO Optoelectronic Materials, Devices and Applications: Conference 7216: Gallium Nitride Materials and Devices IV,* San Jose, CA, USA, January 26–29, 2009.

38. A. Matulionis, "Ultrafast decay of non-equilibrium (hot) phonons in GaN-based 2DEG channels(invited)", ***SIMC-15*** – *Semiconducting and Insulating Materials Conference*,Vilnius, Lithuania, June 15–19, 2009.

39. L. Ardaravičius, J. Liberis, O. Kiprijanovič, M. Ramonas, A. Matulionis, J. Xie, M. Wu, J.H. Leach, and H. Morkoç, "Strain dependent electron drift velocity in $Al_{1-x}In_xN$/AlN/GaN", ***SIMC-15*** – *Semiconducting and Insulating Materials Conference,*Vilnius, Lithuania, June 15–19, 2009.

40. E. Šermukšnis, J. Liberis, and A. Matulionis, "Optimal 2DEG density for plasmon-assisted ultrafast decay of hot phonons", ***ICNF 2009*** – *20th International Conference on Noise and Fluctuations,* Pisa, Italy, June 14–19, 2009.

41. H. Morkoç, Ü. Özgür, and A. Matulionis, „New twists in carrier recombination and hot carrier scattering in light emitting devices and field effect transistors based on III-V nitride semiconductors (invited)", ***2009 Fall EMRS*** – *European Materials Research Society – Meeting*, Warsaw, Poland, September 14–18, 2009.

42. E. Šermukšnis, J. Liberis, and A. Matulionis, "Tuning into plasmon–LO-phonon resonance: gateless two-dimensional channels for nitride HEMTs", *International Commission for Optics Topical Meeting on* ***Emerging Trends & Novel Materials*** *in Photonics*, European Cultural Center of Delphi, Greece, 7–9 October 2009.

43. J. H. Leach, M. Wu, X. Ni, X. Li, Ü. Özgür, H. Morkoç, J. Liberis, E. Šermukšnis, A. Matulionis, and Y.-T. Moon, „Isothermal stress test measurements of lattice matched InAlN/AlN/GaN HFET structures", ***ICNS-8*** – *8th International Conference on Nitride Semiconductors,* ICC Jeju, Korea, October 18-23, 2009.

44. A. Matulionis, J. Liberis, H. Morkoç, "Plasmon-assisted dissipation of LO-mode heat in nitride 2DEG channels", ***SPIE Photonics West,*** *OPTO Optoelectronic Materials, Devices and Applications: Conference 7602: Gallium Nitride Materials and Devices V, San Francisco, CA., USA, January 23–28, 2010.*

45. A. Matulionis, J. Liberis, I. Matulionienė, E. Šermukšnis, J.H. Leach, H. Morkoç, **"**Optimal conditions for heat dissipation in nitride HFETs: Power tunable plasmon–LO-phonon resonance (invited)", ***WOCSDICE 2010 –*** *34th Workshop on Compound Semiconductor Devices and Integrated Circuits held in Europe, Darmstadt/Seeheim, Germany, May 16–19, 2010.*

46. J. Kundrotas, A. Čerškus, J. Liberis, A. Matulionis, J.H. Leach, H. Morkoç, "Enhancement and narrowing of excitonic lines in AlInN/GaN heterostructures", ***UFPS-14*** – *14th International Sympposium on* ***Ultrafast Phenomena*** *in Semiconductors, Vilnius, Lithuania, August 23–25, 2010.*

47. A.Matulionis, J. Liberis, I. Matulionienė, E. Šermukšnis, J. H. Leach, M. Wu, X. Ni, H. Morkoç, "Signatures of hot phonons in reliability of nitride HFETs and signal delay", ***UFPS-14*** *– 14th International Sympposium on* ***Ultrafast Phenomena*** *in Semiconductors, Vilnius, Lithuania, August 23–25, 2010.*

48. L. Ardaravičius, O. Kiprijanovič, and J. Liberis, "Hot-Phonon Decided Carrier Velocity in AlInN/GaN Based Two-Dimensional Channels" ***UFPS-14*** *– 14th International Sympposium on* ***Ultrafast Phenomena*** *in Semiconductors, Vilnius, Lithuania, August 23–25, 2010.*

49. X.Ni, X. Li, J. Lee, S. Liu, V. Avrutin, A. Matulionis, Ü. Özgür, F. Bertram, J. Christen, and H. Morkoç, "Carrier dynamics and the efficiency in InGaN light emitting diodes at high injection levels", ***ISSLED2010*** *– 8th International Sympposium on Semiconductor Light Emitting Devices, , Beijing, China, May 16–21, 2010.*

50. J. H. Leach, M. Wu, H. Morkoç, M. Ramonas, and A. Matulionis. „Heterostructure designs for enhanced performance and reliability in GaN HFETs: Camelback channels" ***SPIE Photonics West****, OPTO Optoelectronic Materials, Devices and Applications: Conference 7939: Gallium Nitride Materials and Devices VI, San Francisco, CA., USA, January 22–27, 2011.*

51. F. Zhang, X. Li, S. Liu, S. Okur, V. Avrutin, Ü. Özgür, and H. Morkoç, A. Matulionis, M. Kisin, „Impact of ballistic electron transport on efficiency of InGaN based LEDs" ***SPIE Photonics West,*** *OPTO Optoelectronic Materials, Devices and Applications: Conference 7939: Gallium Nitride Materials and Devices VI, San Francisco, CA., USA, January 22–27, 2011.*

52. A. Matulionis, M. Ramonas, E. Šermukšnis, J. Liberis, J.H. Leach, M. Wu, and H. Morkoç, "Mitigation of hot-phonon effects in a twin-channel nitride heterostructure field effect transistor", ***WOCSDICE 2011 –*** *35th Workshop on Compound Semiconductor Devices and Integrated Circuits held in Europe, Catania, Italia, May 29–June 1, 2011.*

53. A. Matulionis, M. Ramonas, R. Katilius, S. V. Gantsevich. Theory of fluctuations in non-equilibrium electron–hot-phonon system. ***ICNF 2011*** *– 21st International Conference on Noise and Fluctuations,* Toronto, Canada, June 12 – 16, 2011.

54. A. Matulionis, X. Li, S. Okur, F. Zhang, V. Avrutin, S. J. Liu, Ü. Özgür, H. Morkoç, S. M. Hong, and S. H. Yen, „Effects of hot electrons and active layer design on the quantum efficiency of InGaN LEDs" ***AOMD-7*** *– 7th International Conference on Advanced Optical Materials and Devices,* Vilnius, Lithuania, August 28–31, 2011.

55. L. Ardaravičius, J. Liberis, O. Kiprijanovič, and A. Matulionis, „Hot-electron transport in graded AlGaN alloys" COST Action MP0805: training school: Izmir, Turkey, April 12-14, 2011.

Summary

A novel fluctuation-based approach is applied to consider the unsolved problems in the realm of nitride heterostructure field effect transistors (HFETs). Fluctuations originate at a microscopic level and provide with information on the processes responsible for device operation and degradation. The novel fluctuation-based approach is impelled by recent demonstration of strong correlation of *microwave* hot-electron fluctuations with frequency performance and degradation of nitride HFETs. The correlation has its genesis in the dissipation of the *LO-mode heat* accumulated by the non-equilibrium longitudinal optical phonons (hot phonons) confined in the channel that hosts the high-density hot-electron gas subjected to a high electric field. The LO-mode heat causes additional scattering of hot electrons and facilitates defect formation in a different manner than conventional heat accumulated by acoustic phonons. The heat accumulation depends on the supplied electric power and the rate of heat dissipation. We treat the dissipation problem in terms of the *hot-phonon lifetime* responsible for conversion of non-migrant optical phonons into migrant acoustic modes and other vibrations. The lifetime is measured over wide ranges of electron densities and supplied electric power. The optimal conditions for heat dissipation are determined and are associated with plasmon-assisted disintegration of LO phonons. Signatures of plasmons are experimentally resolved in fluctuations, dissipation, hot-electron transport, transistor frequency performance, transistor phase noise, and device reliability. In particular, a slower degradation and a faster operation of GaN-based HFETs is demonstrated when the plasmon-assisted ultrafast dissipation of the LO-mode heat comes into play. Novel heterostructure designs for improved power conversion efficiency and HFET performance are proposed, implemented, and tested.

1. Introduction

Gallium nitride and related compounds offer attractive solutions for semiconductor electronics and optoelectronics in the frequency range from microwaves to ultraviolet [1,2]. In particular, nitride heterostructure field effect transistors (HFETs) are among the most promising devices for microwave power applications. The main advantage originates from a high-density two-dimensional electron gas (2DEG) located in an undoped semiconductor (GaN) at a heterojunction with a wide band gap semiconductor (AlN and/or its alloys) and operated at a high electric field strength. The main drawbacks are low reliability and rapid drop of the power at millimeter-wave frequencies.

It would be natural to expect a higher microwave power if a higher 2DEG density were confined in a HFET channel [3]. Simultaneously, charging of capacitances would take less time. As a result, a higher power would be combined with a faster operation of HFETs. However, the experimental data do not show the expected behaviour. Figure 1 presents the unity gain cut-off frequency measured for HFETs based on nitride heterostructures that contain different 2DEG density [3–5]. At a given gate length, no increase in the cut-off frequency of the investigated HFETs is observed when the 2DEG density is increased. Experimental study of microwave hot-electron fluctuations suggests a non-traditional explanation of the behaviour in question [6,7].

Fluctuations originate at the microscopic level and provide with information on the processes responsible for device operation, reliability, and failure. The novel fluctuation-based approach is impelled by recent demonstration of strong correlation of microwave hot-electron fluctuations with RF performance and degradation of nitride HFETs [6–8]. The correlation has its genesis in the dissipation of the so-called longitudinal-optical (LO)-mode heat accumulated by the non-equilibrium LO phonons imprisoned in the channel that hosts the high-density hot-electron gas subjected to a high electric field (Fig. 2).

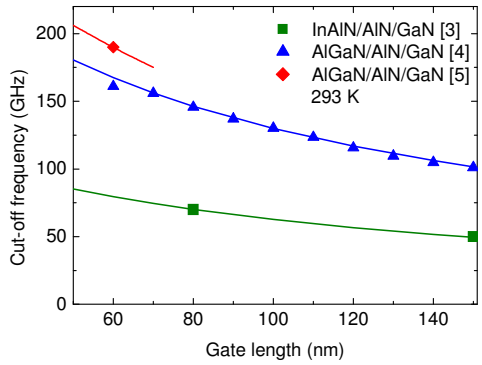

Figure 1 Dependence of cut-off frequency on gate length for GaN HFETs with different 2DEG density in channels: 2.5×10^{13} cm^{-2} (squares [3]), 2.07×10^{13} cm^{-2} (triangles [4]), 1.4×10^{13} cm^{-2} (diamond [5]). At a fixed gate length, cut-off frequency decreases as 2DEG density increases. Curves guide the eye.

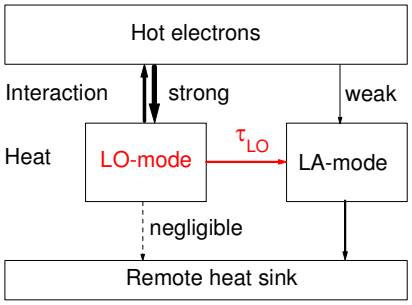

Figure 2 Schematic routes for heat dissipation in a GaN channel. Hot electrons primarily lose their energy through emission of LO phonons. These in turn decay into LA modes before the heat is removed from the channel [10].

At high electric fields, the electrons are displaced from equilibrium and become hot. Because electron–LO-phonon coupling is strong in highly ionic materials, such as GaN, the electrons tend to lose their heat mainly through emission of LO phonons (Fig. 2). The emitted LO phonons remain localized in the channel because their group velocity is very low. As a result, the LO-mode heat is accumulated; it cannot be dissipated or removed from the channel unless the non-equilibrium LO phonons are converted to some other phonon modes with higher group velocities,

for example, longitudinal acoustic (LA) phonons. The conversion of the LO-mode heat into the LA-mode heat can be treated in terms of LO-phonon lifetime. The LO phonon energy exceeds the highest LA energy several times in GaN, and transverse optical (TO) mode is believed to take part through the route LO→TO+LA proposed some time ago [9]. In nitride 2DEG channels, the exact route of LO-phonon decay is not clearly understood but there is compelling experimental [6,10-12] and theoretical [13] evidence that plasmon-assisted process tends to dominate.

Hot-phonon effect is a short term used when accumulation and dissipation of LO-mode heat come into play. Figure 3 illustrates that, at a given applied electric field, the estimated hot-phonon temperature is higher if the 2DEG density is higher [6,14,15]. Since hot phonons cause additional scattering of electrons [16], the accumulation of LO-mode heat has an effect on hot-electron drift velocity and frequency performance of a HFET [7,17]. Data in Figures 1 and 3 are in strong correlation: the frequency performance of the HFETs is worse if the hot-phonon temperature is higher. Mitigating hot-phonon temperature with technological means is an important goal of HFET engineering.

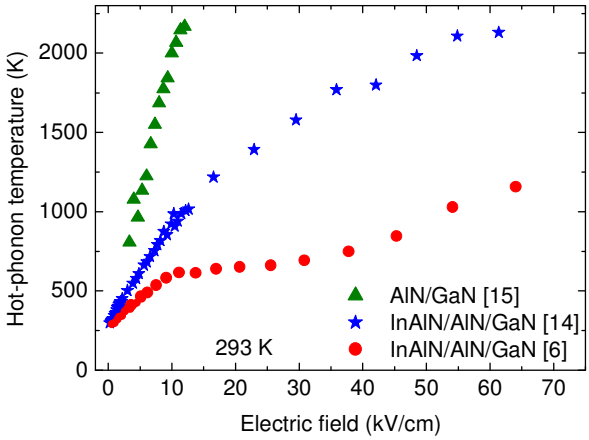

Figure 3 Experimental dependence of hot-phonon temperature on electric field for GaN 2DEG channels with different 2DEG density: $8x10^{12}$ cm^{-2} (bullets [6]), $1.2x10^{13}$ cm^{-2} (stars [14]), $2.5x10^{13}$ cm^{-2} (triangles [15]). At a fixed electric field, hot-phonon temperature increases with 2DEG density.

The project deals with hot-phonon effects in nitride 2DEG channels and HFETs. The unsolved problem of heat dissipation is treated in terms of the hot-phonon lifetime responsible for conversion of the LO-mode heat into migrant modes. Section 2 of the report presents the novel fluctuation–dissipation technique for measurement of hot-phonon lifetime and its approval through comparison of the results with those available from other techniques. The experimental evidence that plasmons assist dissipation of the LO-mode heat is given in section 3. The fluctuation–dissipation technique is demonstrated to be the most powerful way for resolving signatures of plasmon–LO-phonon resonance in 2DEG channels through measuring dependence of the hot-phonon lifetime on the 2DEG density. Section 4 illustrates that the plasmon–LO-phonon resonance can be tuned in, at a fixed 2DEG density, with supplied electric power. The resonance is resolved in experimental data on hot-electron drift velocity measured at a fixed electric field in

gateless channels (Section 5). Tuning into the resonance with gate voltage is illustrated in section 6 together with signatures of the resonance resolved in HFET frequency performance. The signatures of the resonance are resolved in HFET degradation (Section 7). The experimental study of phase noise confirm defect generation during electrical stress (Section 8). Two novel heterostructure designs (a camelback channel and a straircase electron injector) are presented in Sections 9 and 10. The report ends with main conclusions and list of abbreviations and symbols.

2. Methods, Assumptions, and Procedures

Our measurements of hot-phonon lifetime are based on hot-electron fluctuations. Fluctuation-dissipation based technique [16] was developed and implemented after careful analysis of different sources of hot-electron fluctuations in voltage-biased 2DEG channels at microwave frequencies [18,19]. The results on hot-phonon lifetime are available for nitride-based 2DEG channels [6,11,16,20–23], arsenide-based 2DEG channels [24], $SiO_2/Si/SiO_2$ channels [25], and SiC [26]. For recent reviews see [10–12,27–29].

The measurements are carried out on gateless channels supplied with coplanar ohmic electrodes. The technique works best at electric fields and ambient temperatures where the electron–LO-phonon scattering is the dominant electron energy dissipation mechanism. The associated hot-electron fluctuations cause emission of microwave radiation (noise power) detected by a sensitive radiometer. The equivalent noise temperature, or simply noise temperature, is determined from the measured noise power. Pulsed noise power measurements can be made before, during, and after the voltage pulse used to heat the electrons. Short pulses of voltage allow one to control thermal walkout [14,18,21,27,28]. A schematic circuit of the gated radiometric set-up is illustrated in Fig. 4 [14].

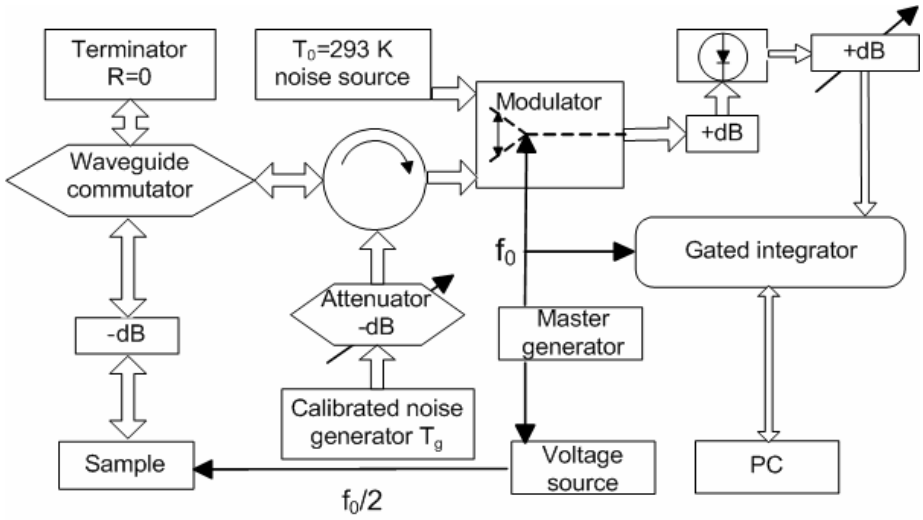

Figure 4 X-band waveguide-type radiometric set-up for pulsed hot-electron noise temperature measurement [14].

The sample is mounted into the waveguide, and the noise temperature is measured in the bias direction at 10 GHz before, during, and after the voltage pulse applied to the sample. The set-up includes JCA812 microwave low noise amplifiers and Stanford Research Systems modules (gated integrator and boxcar averager module SR250, Quad fast amplifier SR240A, and computer interface module SR245). Cascaded wideband (DC–350 MHz) SR240A amplifiers amplify the signal after the microwave detector before the gating. The module SR250 contains an exponential moving averager used for integration of the averaged noise power. The integrator is open for time interval from 10 ns to 10 μs for the integration of the noise power and comparison with the power of the known source of noise. Every second value is inverted before the averager, and the noise power difference is obtained. The averaged noise values are digitized in the computer module SR245 and loaded through RS232 interface to the PC for further averaging. Hand-written Labview software controls the measurements and the data processing. Sample mismatch is taken into account. The measurements include four steps used to obtain the noise temperature together with the sample reflection coefficient and the set-up parameters that include power amplification and additional noise generated by non-ideal waveguide components. The thermal walkout is controlled through measurements before, during, and after the voltage pulse. Recently the setup has been modified to carry out on-wafer measurements; it can operate at different microwave frequencies.

The hot-electron noise temperature $T_n(f)$ is determined from the available noise power $\Delta P_n(f)$ emitted by the hot electrons into a matched load (input of the measurement circuit):

$$T_n(f) = \frac{1}{k_B}\frac{\Delta P_n(f)}{\Delta f} \tag{1}$$

where k_B is the Boltzmann constant and Δf is the frequency bandwidth around the frequency f.

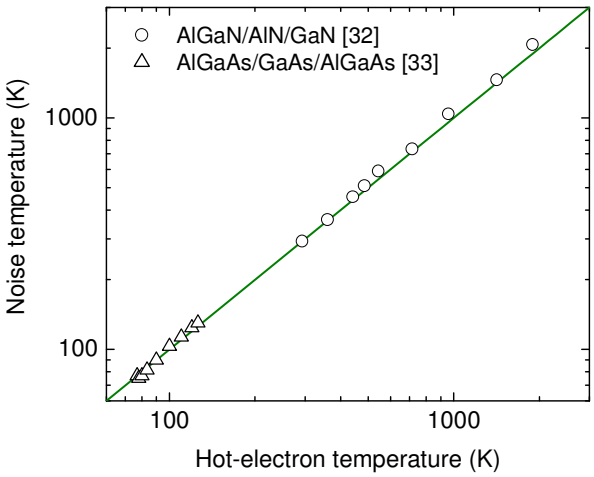

Figure 5 Calculated dependence of noise temperature on hot-electron temperature for 2DEG channels located in AlGaN/AlN/GaN at 300K (circles [32]) and AlGaAs/GaAs/AlGaAs at 77K (open triangles [33]). Line is the hot-electron temperature.

Because of intense electron–LO-phonon interaction in GaN and high density of electrons in a 2DEG channel, the electron temperature can be introduced [30,31]. According to Monte Carlo simulation, the noise temperature T_n is close to the hot-electron temperature T_e [11,32] (Fig. 5, circles and line). A similar conclusion has been earlier reported for AlGaAs/GaAs/AlGaAs 2DEG channels [33] (open triangles). The hot-electron temperature approximation simplifies the theoretic treatment of the hot-phonon problem.

Original fluctuation technique estimates the hot-phonon lifetime τ_{LO} according to the Arrhenius-type expression for the dissipated power P_d [16]:

$$P_d = \frac{\hbar\omega_{LO}}{\tau_{LO}} \exp(-\frac{\hbar\omega_{LO}}{k_B T_e}) \tag{2}$$

where $\hbar\omega_{LO}$ was the LO-phonon energy. Expression (2) fitted the experimental data in the range of not too high electron temperatures [16]. The fitted activation energy equaled the LO-phonon energy; this confirmed that acoustic phonons played a negligible role in the electron energy dissipation. Thus, the electron–LO-phonon interaction was the dominant electron energy dissipation mechanism (Fig. 2). Under steady-state conditions, the dissipated power equaled the supplied power: $P_d = P_s$. In a voltage-biased channel, the supplied electric power per electron was:

$$P_s = \frac{UI}{N_{el}} \tag{3}$$

where U is the applied voltage, I is the current, and N_{el} is the number of electrons in the channel.

A more sophisticated way for estimating the hot-phonon lifetime is based on estimation of equivalent hot-phonon temperature [20, 23, 28]. When the electron–LO-phonon interaction is the dominant electron energy dissipation mechanism, the hot-electron energy dissipation rate, or the dissipated power, is determined by the temperatures of hot electrons and hot phonons, T_e and T_{LO}. The electron energy dissipation includes spontaneous and stimulated emission of LO phonons by high-energy electrons and re-absorption of LO phonons by all electrons. Let us introduce equivalent occupancy N_{LO} of the involved hot-phonon modes and express the power dissipated by an average electron as follows [34]:

$$P_d = \frac{\hbar\omega_{LO}}{\tau_{sp}}(1 + N_{LO})p^- - \frac{\hbar\omega_{LO}}{\tau_{abs}} N_{LO} p^+ \tag{4}$$

where τ_{sp} is the mean time for spontaneous emission of an LO-phonon by a high-energy electron, τ_{abs} is the mean time for LO-phonon absorption by any of the electrons (the time "constants" τ_{sp} and τ_{abs} demonstrate weak variation with the electron energy), and the probabilities $p^{\pm}$ to find an electron ready either to emit (–) or absorb (+) an LO phonon are:

$$p^{\pm} = \int D(\varepsilon) f(\varepsilon)[1 - f(\varepsilon \pm \hbar\omega_{LO})] d\varepsilon / n_{2D} \tag{5}$$

where ε is the electron energy, D is the density-of-states function, $f(\varepsilon)$ is the electron-temperature-dependent Fermi–Dirac distribution function, and n_{2D} is the 2DEG density (the sheet electron density in the 2DEG channel).

The occupancy N_{LO} is obtained from Eq. (4) and the balance equation $P_d = P_s$; the equivalent hot-phonon temperature T_{LO} is estimated according to Bose–Einstein function. Squares and bullets in Fig. 6 illustrate that, for a GaN 2DEG channel, the equivalent hot-phonon temperature is close to the hot-electron temperature (line); this behaviour is typical for an almost isolated hot electron–LO-phonon subsystem under intense exchange of energy between the electrons and the LO phonons [16].

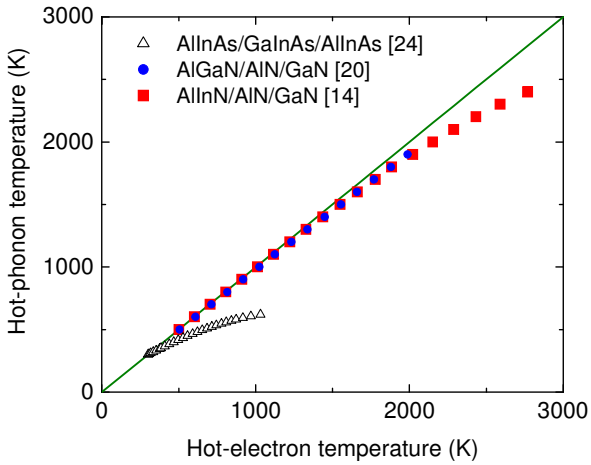

Figure 6 Experimental dependence of equivalent hot-phonon temperature at room temperature for 2DEG channels located in AlInAs/GaInAs/AlInAs (triangles [24]), AlInN/AlN/GaN (squares [14]), and AlGaN/AlN/GaN (bullets [20]). Line is the hot-electron temperature.

The experimental data on 2DEG channels confined in GaN (Fig. 6, closed symbols) are compared with those for AlInAs/GaInAs/AlInAs structure with the 2DEG channel confined in the InGaAs layer (open triangles). Thelatter structure demonstrates a weaker coupling inside the hot electron–LO-phonon subsystem, as compared with the GaN structures, and the estimated hot-phonon temperature is up to 30% lower (Fig. 6, triangles) than the hot-electron temperature (line) [24].

Because of strong coupling inside the hot subsystem in the GaN heterostructures, the hot electrons and the hot-phonons demonstrate close temperatures and relax together. In other words, the corresponding relaxation time constants acquire comparable values [20]:

$$\tau_{LO} \approx \tau_{\varepsilon} \qquad (6)$$

where τ_{ε} is the hot-electron energy (temperature) relaxation time. Consequently, the hot-phonon lifetime can be estimated after Eq. (6) if the hot-electron energy relaxation time is measured. The hot-electron energy relaxation time, τ_{ε} , can be determined from the noise experiment [18–20]:

$$\tau_\varepsilon = k_B \frac{dT_e}{dP_s} \tag{7}$$

Another way for estimating the hot-phonon lifetime follows from the dependence of the hot-phonon mode occupancy N_{LO} on the supplied electric power P_s (for experimental data see symbols in Figure 7). The required dependence, $N_{LO}(P_s)$, can be obtained from the experimental dependence of the hot-electron temperature on the supplied power as described earlier in this report (see also [11, 20]). The effective dynamic hot-phonon lifetime is introduced as follows [11]:

$$\tau_{LO} = \hbar\omega_{LO} \frac{dN_{LO}}{dP_s} \tag{8}$$

For GaN 2DEG channels, the power-independent hot-phonon lifetime is obtained at a low occupancy of hot-phonon states: $N_{LO} < 0.4$ (Fig. 7, solid lines). The fitting of the experimental data is reasonably good. Blue line stands for the value τ_{LO} = 300 fs; this value is ~25% lower than the hot-electron energy relaxation time estimated according to Eq. (8) for the same AlGaN/AlN/GaN structure [20].

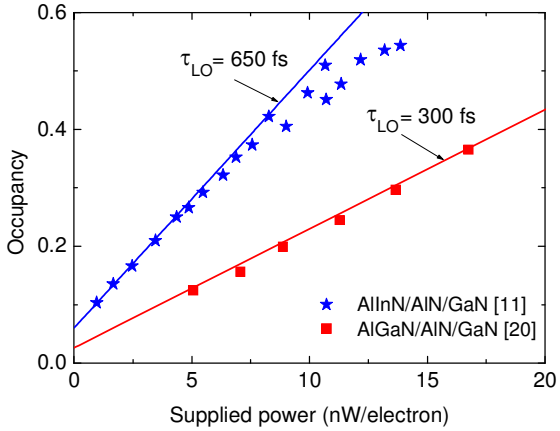

Figure 7 Dependence of hot-phonon mode occupancy on supplied electric power for 2DEG channels: AlGaN/AlN/GaN (squares, after [20]) and InAlN/AlN/GaN (stars [11]). Fitted lines stand for τ_{LO}= 300 fs (blue) and τ_{LO} = 650 fs (red).

The definition of the dynamic hot-phonon lifetime, Eq. (8), becomes of special importance when the lifetime depends on supplied power. The corresponding experimental data for GaN 2DEG channels [6, 10, 11, 23, 28] will be discussed later.

Red line in Figure 8 shows the hot-phonon decay for AlGaN/GaN 2DEG channel subjected to low–moderate electric field when the hot-phonon lifetime is estimated from hot-electron fluctuations [16]. In an independent experiment, the hot phonons are injected into the AlGaN/GaN 2DEG channel by a femtosecond laser pump pulse, and intersubband absorption is measured by the probe beam delayed with respect to the pump pulse. The hot phonons assist intersubband electron

transitions, and the probe beam is absorbed when the phonons are present in the channel (Fig. 8, stars [35]). The estimated hot phonon lifetime, 380 fs [35], is in good agreement with the pioneering result for a similar AlGaN/GaN 2DEG channel obtained from fluctuations, 350 fs [16].

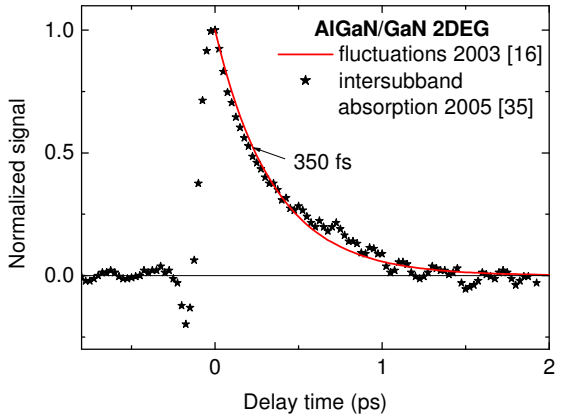

Figure 8 Intersubband absorption (stars [35]) and hot-phonon decay (line [16]) in AlGaN/GaN 2DEG channel.

The time-resolved pump–probe Raman experiment is the most reliable way for measuring the hot-phonon lifetime [36]. Some results are shown in Figure 9 for bulk GaAs and GaN (opens symbols, [36, 37]).

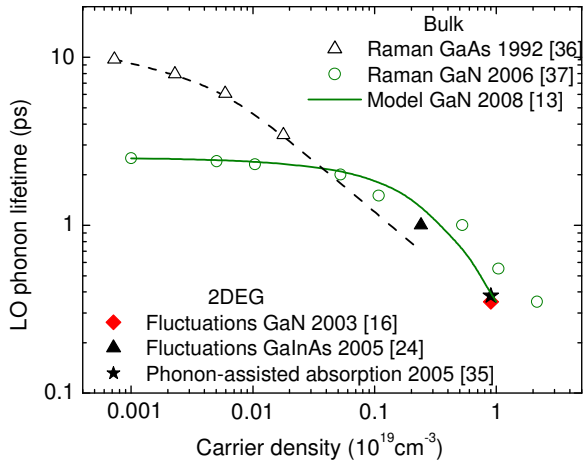

Figure 9 Monotonous decrease of hot-phonon lifetime when carrier density increases. Raman data (open symbols): GaAs (open triangles [36]) and GaN (open circles [37]). Fluctuations and inter-subband absorption (closed symbols): AlGaN/GaN (red diamond [16], star [35]) and AlInAs/GaInAs/AlInAs (triangle [24]). Solid curve is plasmon model for GaN [13]. Dashed curve guides the eye.

In the Raman experiment, photons of the probe beam are scattered by the hot phonons injected earlier by the pump pulse of a femtosecond laser. The intensity of scattered light depends on time delay of the probing with respect to the pump pulse. The hot-phonon lifetime is obtained from relaxation of intensity of the anti Stokes line associated with the decrease of the number of hot phonons as they decay into other modes. However, Raman experiments are difficult to carry out on a single 2DEG channel of nanometric thickness, and no hot-phonon lifetime datum is available from Raman experiments for the voltage-biased 2DEG channels that contain a high density of electrons at equilibrium and are used for HFET fabrication.

According to the Raman data for bulk GaAs [36] and bulk GaN [37], the hot-phonon lifetime monotonously decreases as the electron–hole density increases (Fig. 9, open symbols). The fluctuation-based result for AlInAs/GaInAs/AlInAs 2DEG (closed triangle [24]) is in a reasonable agreement with the extrapolated dependence on the carrier density (dashed curve) measured for GaAs by the Raman pump–probe technique (open triangles [36]). The results for bulk GaN (open circles [37]) are close to those (star, diamond [16,31]) for the AlGaN/GaN 2DEG channels when the electron density per unit volume is estimated as the sheet 2DEG density divided by the quantum well width at the Fermi energy [22]. Consequently, the fluctuation–dissipation technique is suitable for reaching the goals of the project: the technique can measure dependence of hot-phonon lifetime on electron density [6,10–12] over a wide range of 2DEG densities.

Nominally undoped InAlN/AlN/GaN gateless structures and HFETs for this project were grown on c-plane semi-insulating GaN:Fe substrates (with a bulk resistivity of ~10^9Ω-cm) in a low-pressure custom-designed organo-metallic vapor phase epitaxy (OMVPE) system at Virginia Commonwealth University (Richmond, VA) [6–8,23]. The growth was initiated with a 250 nm AlN nucleation layer, and followed with a 2–4 μm thick undoped GaN layer, a 1-nm-thick undoped AlN spacer layer, and a 18-nm-thick undoped InAlN barrier layer, and finally a ~2-nm-thick GaN cap layer. Trimethyl-gallium, trimethyl-aluminum, and ammonia were used as the Ga, Al, and N sources, respectively. The 2DEG channel was located in the undoped GaN layer close to the AlN spacer. Coplanar ohmic Ti/Al/Ni/Au electrodes were annealed at 1120 K. For HFETs, a standard liftoff procedure was used to define source and drain contacts, to etch mesas for isolation, and to deposite Pt/Au gate contacts. X-ray diffraction was used to confirm the barrier layer thickness and composition.

In order to mitigate deleterious hot-phonon effects, a novel heterostructure with camelback electron density profile in the channel has been proposed [39]. The grown and tested heterostructures contain a composite $Al_{0.1}Ga_{0.9}N$/GaN channel embedded into the heterostructure between the undoped GaN layer and the AlN spacer (Figure 10). The barrier alloy layer of $Al_{0.82}In_{0.18}N$ is overgrown above the AlN spacer. The camelback channel structure was grown on a sapphire substrate in the same OMVPE system at Virginia Commonwealth University [38]. The structure consisted of a low temperature AlN buffer layer followed by 2 μm of GaN, a 2 nm $Al_{0.1}Ga_{0.9}N$ sub-channel, a 1 nm AlN spacer, and a (18–20) nm $Al_{0.82}In_{0.18}N$ barrier layer. The Schottky diodes were used for capacitance–voltage measurements to assess the total charge density of the mobile electrons (2DEG density) and the electron 3D density profile. The TLM patterns were used for microwave noise analysis to assess the hot-phonon lifetime. In these measurements, the noise temperature is measured as a function of power supplied during the voltage pulse [16].

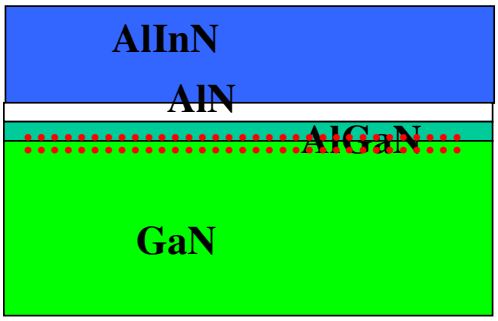

Figure 10 Schematic view of a heterostructure with the camelback channel located below the AlN spacer (white) and shared by the $Al_{0.1}Ga_{0.9}N$ layer (light blue) and the GaN layer (green). The mobile electrons (red symbols) are embedded in the camelback channel. The 2DEG density is controlled by the AlInN barrier (dark blue).

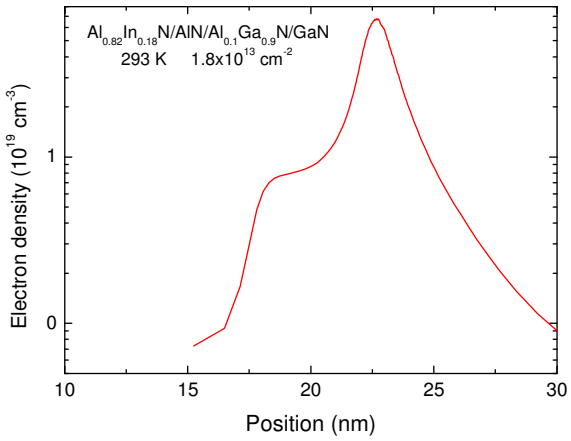

Figure 11 Electron 3D density profiles measured by capacitance–voltage technique for the camelback channel located inside $Al_{0.82}In_{0.18}N/AlN/Al_{0.1}Ga_{0.9}N/GaN$ structure [38].

Figure 11 illustrates the electron density profile measured by the capacitance–voltage technique for the composite channel shown in Fig. 10. The electron density per unit volume approaches 7 10^{19} cm^{-3} inside the GaN layer where the main peak is located. Some electrons occupy the sub-channel in the $Al_{0.1}Ga_{0.9}N$ layer and form the left-hand shoulder of the profile at room temperature. According to Schrödinger–Poisson calculations, the peak density decreases, and the secondary peak develops inside the $Al_{0.1}Ga_{0.9}N$ sub-channel at elevated hot-electron temperatures [38]. Thus, the composite structure exhibits a "camelback" electron density profile under electron heating with electric field. The camelback profile is expected to have a lower bulk electron density as compared with that in the standard $Al_{0.82}In_{0.18}N/AlN/GaN$ channel supposing that the 2DEG density (sheet density) is kept the same.

3. Plasmon-Assisted Resonance Decay of Hot Phonons

The monotonous decrease of the lifetime with the increase in the electron density (Fig. 9, circles [37]) can be explained within the plasmon–LO-phonon model developed for GaN (Fig. 9, solid curve [13]). According to the model, the hot-phonon lifetime decreases when the plasmon frequency increases and approaches the LO-phonon frequency.

For an infinite electron plasma, the frequencies of uncoupled modes of plasmons and LO phonons would cross at the 3DEG electron density

$$n_{cr} = \omega_{LO}^2 \frac{m_e^* \varepsilon}{e^2} \tag{9}$$

where $\hbar\omega_{LO}$ is the LO-phonon frequency at zero electron density and ε is the dielectric constant. The coupled modes become most important at the crossover electron density, near 10^{19} cm^{-3} in bulk GaN.

Supposing that the fastest decay of hot phonons is expected in the vicinity of the crossover and the range of electron densities is wide enough, a non-monotonous resonance-type dependence of the hot-phonon lifetime on the density can be predicted. While the Raman data demonstrate a monotonous decrease in the investigated range of carrier densities (Fig. 9, open symbols), a strong argument in favour of plasmon-assisted decay of hot phonons could be obtained from experimental data on the lifetime at electron densities above the plasmon–LO-phonon crossover. However, no lifetime datum is available for GaN, GaAs, and other compound semiconductors. On the other hand, Table 1 illustrates that the fluctuation technique can measure the lifetime in nitride heterostructures in the range of electron densities below and above the crossover density [22].

Table 1 Nitride heterostructures with 2DEG channels located in GaN [11]

Barrier mole ratio, %			Spacer	2DEG density 10^{13}cm^{-2}	Hot-phonon lifetime, fs	Reference
Al	In	Ga				
15	--	85	none	0.5	350	[16]
22	--	78	GaN/AlN	0.5	140	[42]
33	--	67	AlN	1.0	450	[20]
82	18	--	AlN	0.8	270	[6]
82	18	--	AlN	1.2	650	[28]
82	18	--	AlN	1.5	1000	[11]
82	18	--	AlN	1.5	1500	[11]

Figure 12 presents the data of Table 1 for the nitride heterostructures (closed symbols) together with the Raman data for bulk GaN (open circles). The experimental results of Figure 12 on the heterostructures can be approximated with a simple resonance curve (solid line) [12, 42, 43]:

$$\tau = a\left[1 + \frac{b}{\left(\sqrt{n_{2D}} - \sqrt{n_{res}}\right)^2 + c}\right]^{-1} \tag{10}$$

where n_{2D} is the 2DEG density and n_{res} is the resonance 2DEG density for the fastest decay of hot phonons. The fitted resonance density is ~7 x 10^{12} cm^{-2}.

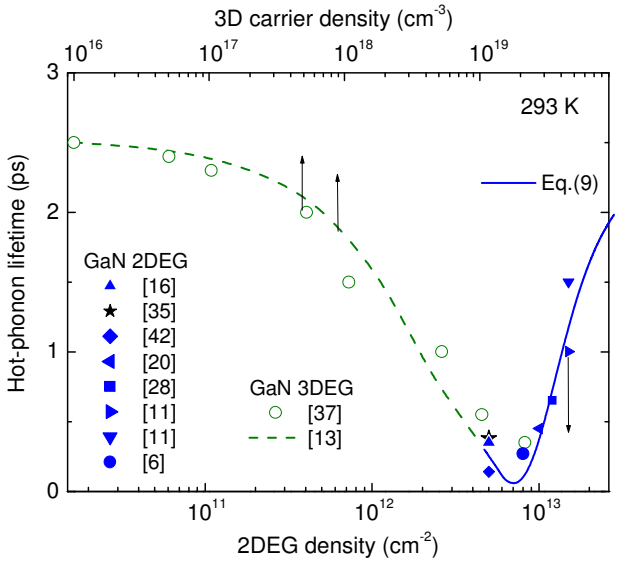

Figure 12 Non-monotonous dependence of hot-phonon lifetime on electron density in GaN-based 2DEG channels (closed symbols): intersubband absorption (star [35]), and fluctuations (blue symbols). Solid curve is Eq. (10). Circles stand for GaN (top scale, Raman data [37]), dashed curve is plasmon model for GaN [13].

An additional argument in favour of the plasmon-assisted decay can be obtained through comparison of the results for nitride and arsenide 2DEG channels [11]. Let us estimate average 3DEG density as the 2DEG density divided by the quantum well width at the Fermi energy [22]. Now, according to Eq. (9), the crossover would take place at a lower 2DEG density in the arsenide channels because of lower electron effective mass and lower LO-phonon energy. The only result on hot-phonon lifetime was available for the GaInAs 2DEG channel at sheet density of 2.3x10^{12} cm^{-2} [24] (Fig. 9, closed triangle). However, after Eq. (6), valid when hot-phonon decay bottlenecks the hot-electron energy relaxation [24], the data on the energy relaxation for different arsenide heterostructures with 2DEG channels can be used to illustrate the plasmon effect [18]

Table 2 Arsenide heterostructures with 2DEG channels located in $Ga_{1-x}In_xAs$

x	Composition	2DEG density $10^{13}cm^{-2}$	Reference
67	$InP/Ga_{1-x}In_xAs/ InP$	0.17	[18]
80-53	$Al_{0.48}In_{0.52}As/Ga_{1-x}In_xAs/ Al_{0.48}In_{0.52}As/InP$	0.15	[18]
70/53	$Al_{0.48}In_{0.52}As/Ga_{1-x}In_xAs/ Al_{0.48}In_{0.52}As/InP$	0.23	[18]
53	$Al_{0.48}In_{0.52}As/Ga_{1-x}In_xAs/ Al_{0.48}In_{0.52}As/InP$	0.24	[18]
70	$Al_{0.48}In_{0.52}As/Ga_{1-x}In_xAs/ Al_{0.48}In_{0.52}As/InP$	0.41	[18]
53	$Al_{0.48}In_{0.52}As/Ga_{1-x}In_xAs/ Al_{0.48}In_{0.52}As/InP$	3.0	[43]

The green bullets in Figure 13 show the data for the arsenide channels listed in Table 2. The green curve is Eq. (10), where n_{res} = 2.7x10^{12} cm^{-2}. while the red curve stands for 6.5x10^{12} cm^{-2}. As expected, a lower crossover 2DEG density is observed in the arsenide 2DEG channels (green curve and bullets) as compared with their nitride counterparts (red curve and squares). Of course, the resonance 2DEG density does not coincide with the crossover 2DEG density where the plasmon–LO-phonon dispersion curves cross, but the expected shift of the resonance position is clearly shown.

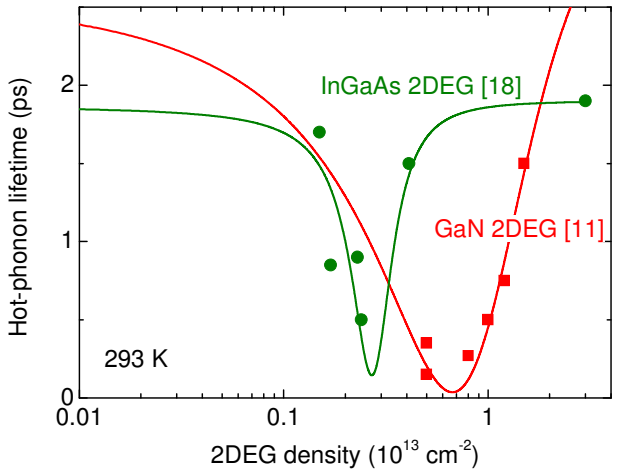

Figure 13 Resonance-type dependence of hot-phonon lifetime on 2DEG density for channels confined in GaN (red squares [11]) and InGaAs (green bullets [18]). For references see Tables 1 and 2. Solid curves illustrate Eq. (10).

In conclusion, Figure 13 presents a convincing experimental evidence for plasmon-assisted dissipation of hot-electron energy through the route discussed in relation with Figure 2. The fluctuation technique proves to be a suitable technique for experimental study of the dissipation in 2DEG channels in terms of hot-phonon lifetime.

4. Power-Tuned Resonance Decay of Hot Phonons

The Schrödinger–Poisson calculations show that the electron density profile depends on the hot-electron temperature in the 2DEG channel (Fig. 14) [10]. There is no simple expression for the plasmon frequency for arbitrary electron density profile, but one can expect, after Fig. 14 and Eq. (9), that the plasma frequency decreases when the peak three-dimensional density decreases as the electron gas expands under heating. As discussed in Section 3, plasmons assist conversion of LO phonons into LA phonons, and the fastest decay of hot phonons takes place in the vicinity the plasmon–LO-phonon crossover. Consequently, the electron heating changes the position of the crossover on the 2DEG density scale, and the resonance 2DEG density shifts with the electron temperature [6]. Let us estimate the shift in two ways.

In the first way, the calculated peak value of the electron 3DEG density profile is kept independent of the electron temperature when a higher 2DEG density is chosen at a higher electron temperature (Fig. 15, open circles) [41]. As a result, the slope of 2.7×10^9 $cm^{-2}K^{-1}$ is obtained (Fig. 15, green line and open circles). The result of the calculation can be compared with the experimental shift of the resonance.

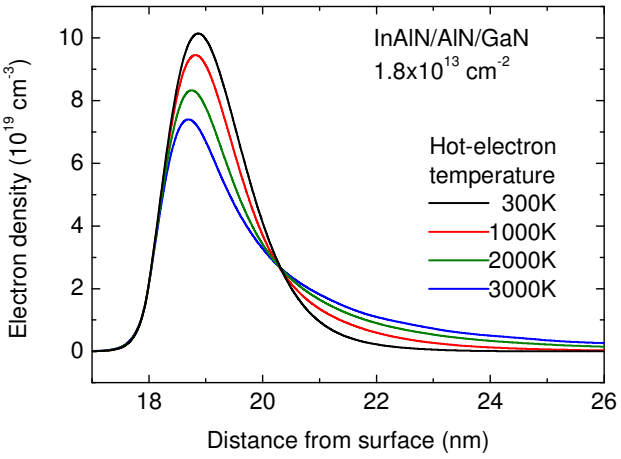

Figure 14 Calculated electron density profile in an InAlN/AlN/GaN structure at different hot-electron temperatures: 300 K (black curve), 1000 K (red curve), 2000 K (green curve), and 3000 K (blue curve) [10].

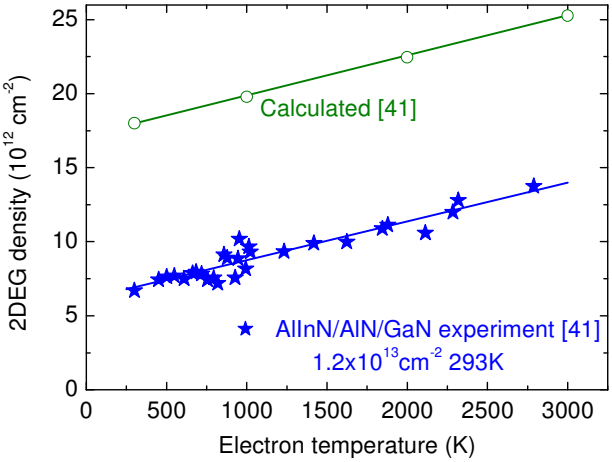

Figure 15 Dependence on hot-electron temperature of resonance 2DEG density (stars), and the 2DEG density required to keep the peak electron density unchanged under thermal expansion of 2DEG gas (circles) [41].

The experimental shift of the resonance 2DEG density with the supplied power can be estimated from the power-dependent hot-phonon lifetime. Figure 16 shows the experimental data on the lifetime for an AlInN/AlN/GaN structure obtained according to Eq. (8) from the power-dependent occupancy of the hot-phonon modes [10]. At a low supplied power, the lifetime is almost independent of the power (Figs. 7, 16), but essential changes develop at high supplied powers. The results of Fig. 16 illustrate that the lifetime decreases from the low-power value of above ~600 fs and reaches ~60 fs as the hot-electron temperatures increases above 2000 K [10]. According to the blue line, the shortest hot phonon lifetime is observed at ~2400 K if the 2DEG density is $1.2x10^{13}cm^{-2}$.

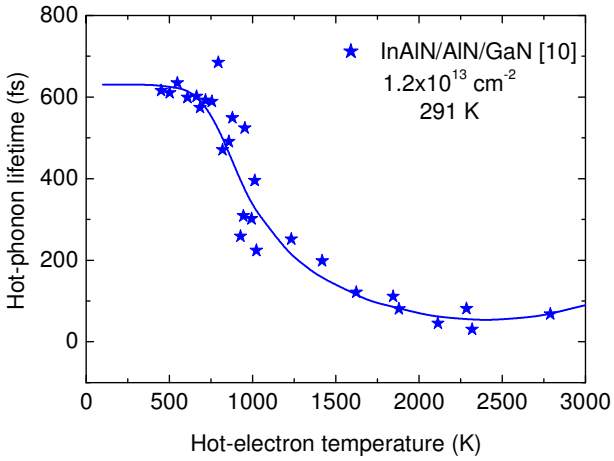

Figure 16 Experimental dependence of hot-phonon lifetime on hot-electron temperature for AlInN/AlN/GaN structure with 2DEG channel subjected to electric field (stars [10]). The 2DEG density is $1.2x10^{13}cm^{-2}$. Curve guides the eye.

In order to obtain the dependence of the resonance 2DEG density on the hot-electron temperature from the experimental data of Fig. 16, we have used the following procedure [41]. Each value of the lifetime (stars in Fig. 16) is fitted with the resonance-type expression given by Eq. (10) where the coefficients *a, b,* and *c* are assumed independent of the hot-electron temperature. The fitting yields the dependence of the resonance 2DEG density on the hot-electron temperature shown in Fig. 15 (stars). Blue line in Fig. 15 is drawn for $2.6x10^{9}$ $cm^{-2}K^{-1}$. The slope of the shift of the resonance 2DEG density (Fig. 15, blue line, stars) is close to the shift estimated from the Schrödinger–Poisson calculations (green line, circles).

The results of Figures 15 and 16 suggest that the resonance can be tuned in, at a given 2DEG density, with the hot-electron temperature that depends on the supplied power. As discussed, the temperature for the resonance is 2400 K at the 2DEG density of $1.2x10^{13}$ cm^{-2} (Fig. 15, blue line). This result is of fundamental rather than practical importance because high electron temperatures cause damage. However, the resonance hot-electron temperature is easy to reach in experiment if the 2DEG density is closer to the resonance 2DEG density of ~$6.5x10^{12}$ cm^{-2} estimated at a low supplied power (Fig. 13, red curve). The blue line in Fig. 15 helps to estimate the resonance

temperature as ~700 K when the 2DEG density is $8x10^{12}$ cm^{-2}. This possibility is demonstrated in Fig. 17 where the minimum value for the lifetime of ~30 fs is reached at the resonance power of ~20 nW/electron corresponding to the hot electron temperature of ~700 K [6].

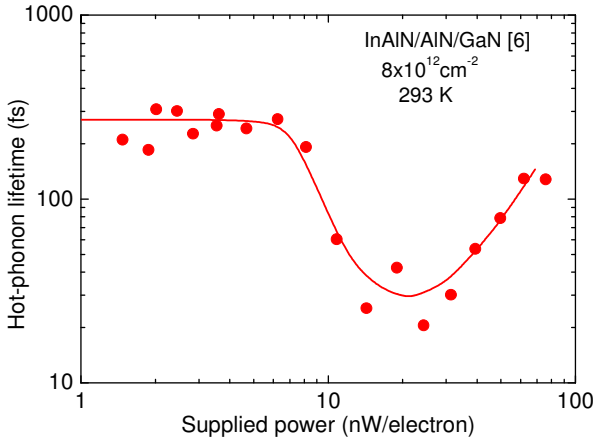

Figure 17 Experimental dependence of hot-phonon lifetime on supplied power for AlInN/AlN/GaN structure (bullets [6]). The 2DEG density is $8x10^{12}cm^{-2}$. Line guides the eye.

To reiterate, the fluctuation technique is the way for observing the plasmon–LO-phonon resonance that is tuned in with the electric power supplied to a 2DEG channel. The tuning with the supplied power is a new way for achieving the ultrafast dissipation of the LO-mode heat [11].

5. Signature of the Resonance: Drift Velocity

Monte Carlo simulation of hot-electron transport shows that a longer hot-phonon lifetime introduces a stronger scattering of electrons and causes a lower drift velocity (Fig. 18) [16]. In particular, the LO-phonon emission rate by an electron increases in proportion with $1+N_{LO}$, and the LO-phonon absorption rate increases proportional to N_{LO} where N_{LO} is the occupancy of the hot-phonon modes responsible for the scattering. When an event of emission of an LO phonon is followed with an absorption event of another LO phonon, the resultant change in the electron energy is negligible, but the direction of motion changes considerably; as a result, the electron drift velocity reduces. A shorter hot-phonon lifetime leads to a lower occupancy N_{LO} and a higher drift velocity as demonstrated through the Monte Carlo simulation (Fig. 18, blue stars, [16]). Consequently, at a fixed electric field, the electron drift velocity is expected to depend on the 2DEG density in a non-monotonous way that can be approximated with the resonance-type dependence, similar to an inverted Eq. (10).

The nanosecond-pulsed current–voltage technique was applied to study hot-electron transport along the two-dimensional electron gas channels confined in nominally undoped AlInN/AlN/GaN structures each supplied with two coplanar ohmic electrodes [44]. The hot-electron drift velocity was deduced under the assumptions of uniform longitudinal electric field and field-independent

electron sheet density. At a fixed electric field, a resonance-type non-monotonous dependence of the velocity on the electron density was found and approximated with the simple resonance curves obtained according to inverted Eq. (10) (Fig. 19a, symbols and red curves). The peak velocity increases from 1.1 to 2.3 10^7 cm/s, and the resonance position shifts from 1.1 to 1.2 10^{13} cm^{-2} when the electric field increases from 20 kV/cm to 80 kV/cm, respectively.

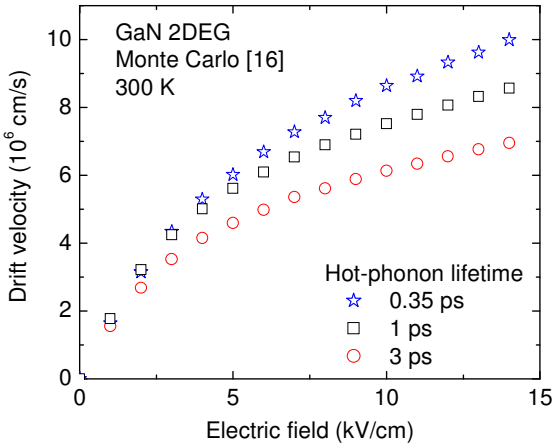

Figure 18 Simulated dependence of hot-electron drift velocity on applied electric field for AlGaN/GaN 2DEG channel [16].

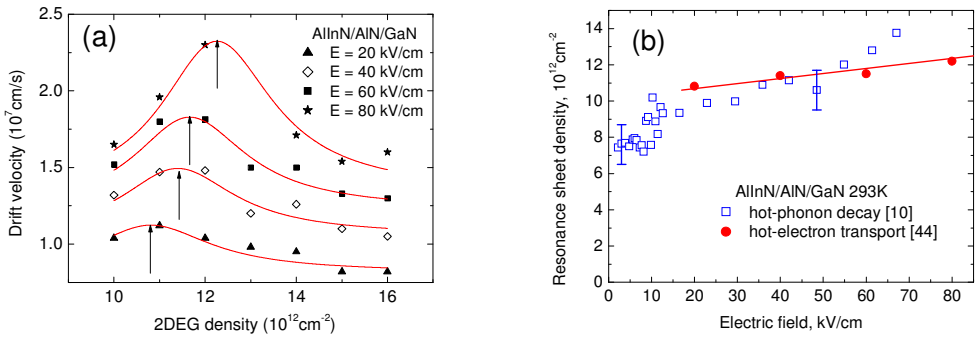

Figure 19 Experimental dependences (a) of hot-electron drift velocity on electron density at a fixed applied electric field and (b) on electric field of the resonance 2DEG density obtained from hot-phonon lifetime experiment (blue squares [10]) and hot-electron drift velocity experiment (red bullets [44]) for AlGaN/AlN/GaN structures.

Figure 19b compares the resonance positions, obtained from the independent experiments on hot-phonon lifetime (blue squares) and hot-electron drift velocity (red bullets). The both techniques yield similar results at 40 kV/cm electric field. Though the shift of the resonance with electric field has slightly different slopes, the plasmon-assisted resonant behavior is demonstrated in two independent experiments.

6. Signature of the Resonance: HFET Frequency Performance

The study of hot-electron transport and microwave fluctuations puts a solid background for considering heat dissipation in HFETs. It has been demonstrated that the ultrafast decay of LO-mode heat causes a lower occupancy of the hot-phonon modes, a weaker scattering due to hot-phonons, and a higher electron drift velocity. This takes place when the 2DEG density approaches the plasmon–LO-phonon crossover and the associated resonance comes into play. Our next goal is to resolve signatures of the resonance in HFET performance. The resonance can be approached in several ways, at least: (i) since the 2DEG density depends on the heterostructure design, the resonance condition can be satisfied during heterostruture growth (ii) supposing that the 2DEG density in the channel exceeds the resonance value at low electric fields, the channel can be tuned into the resonance through heating of the electron gas, (iii) in a HFET, the electron density can be controlled by the gate voltage while the drain voltage can be kept constant to maintain the same electric power supplied to an average electron.

Experiments on HFETs yield the electron drift velocity through measurement of the signal delay extracted from the unity-gain cut-off frequency. The delay originates, in part, from intrinsic transit time needed for the electrons to pass the high-field region located under the gate in the channel. Figure 20 illustrates the results on the intrinsic transit time extracted from the unity gain cut-off frequency measured at a fixed drain bias for an InAlN/AlN/GaN HFET [7].

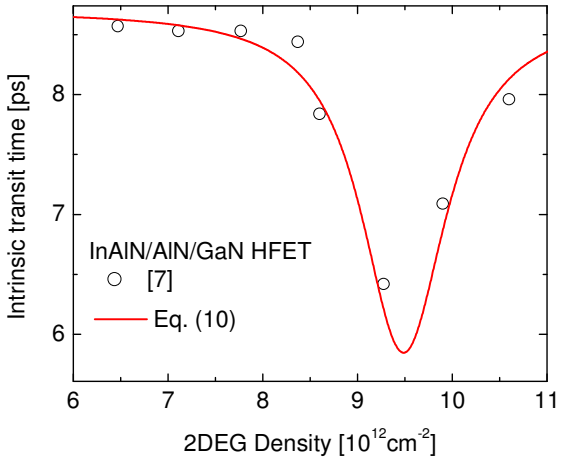

Figure 20. Dependence of intrinsic transit time on 2DEG density for InAlN/AlN/GaN HFETs (circles [7]) and Eq. (10) for $n_{res} = 9.5 \cdot 10^{12}$ cm^{-2} (curve).

On-wafer microwave measurements in frequency range from 2 to 20 GHz were carried out with an HP8510B vector network analyzer. The S-parameters were collected under many dc bias conditions and subsequently were used to compute the small signal current gain, H21. By collecting small signal current gain cutoff frequencies at various bias conditions, we were able to perform Moll's transit time analysis [44]. Figure 20 illustrates the intrinsic transit time for

InAlN/AlN/GaN HFETs when the 2DEG density is controlled with the gate voltage (circles [7]). The results show the signature of the resonance at the 2DEG density of n_{res} = 9.5x10^{12} cm^{-2} as evidenced through fitting the results with Eq. (10) (Fig. 20, curve). The fitted resonance 2DEG density (Fig. 20, curve) together with the results of Fig. 15 (blue line, stars) allows one to estimate the hot-electron temperature in the channel under the gate: the estimated temperature is ~1200 K.

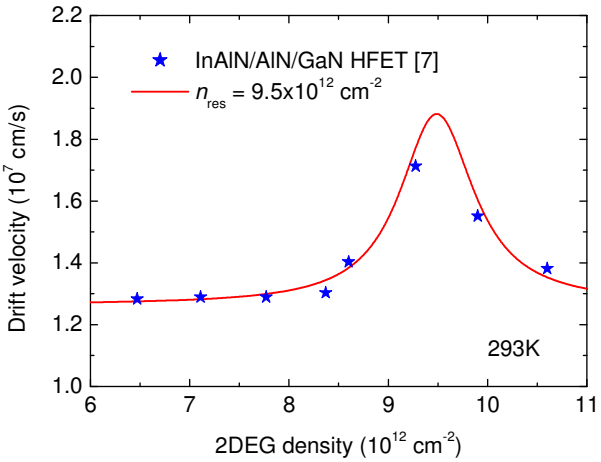

Figure 21 Dependence of electron drift velocity on 2DEG density for InAlN/AlN/GaN HFET (stars [7]). Solid curve is inverted Eq. (10) for n_{res} = 9.5x10^{12} cm^{-2} .

The intrinsic transit time yields the hot-electron drift velocity (Fig. 21). The non-monotonous dependence on the 2DEG density is in a qualitative agreement with the results obtained for gateless heterostructure channels (Fig. 19a). The enhancement of the drift velocity correlates with the resonance obtained in the independent hot-phonon lifetime experiment (Fig. 13) if the shift of the resonance with the hot-electron temperature is taken into account (Fig. 15).

Since the effect of hot phonons is deleterious for device performance, we propose that optimal performance can only be expected when the device is operating under the optimal bias conditions in which the 2DEG density associated with the given bias condition is congruent with the value associated with the shortest hot-phonon lifetime.

7. Signature of the Resonance: HFET Degradation

In a similar way, the signature of the resonance was resolved in an independent experiment on device degradation [8]. High electric field stress measurements were carried out at room temperature on a set of InAlN/AlN/GaN HFETs. The degradation of drain current in InAlN/AlN/GaN HFETs was caused by a fixed amount of charge transported along the channel at a fixed drain voltage (Fig. 22, stars). The degradation as a function of the average electron density in the GaN channel (as determined by gated Hall bar measurements for the particular gate biases used), has a minimum for electron densities around 1 x 10^{13} cm^{-2}, and tends to follow the hot-

phonon lifetime dependence on electron density (Fig. 22, curve). The observations are consistent with the buildup of hot phonons and their ultrafast decay. The resonances appear at about the same electron density in the gateless 2DEG channel when the shift of the resonance with the hot-electron temperature is taken into account in the discussed way (see Figs. 15, 19).

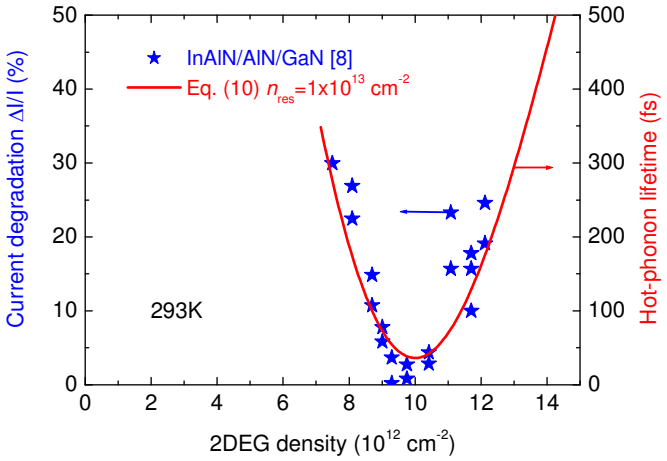

Figure 22 Drain current degradation of InAlN/AlN/GaN HFETs (stars [8]) correlates with hot-phonon lifetime (curve). Curve is Eq. (10) when n_{res} = 1x10^{13} cm^{-2}.

The hot-electron temperature in the channel under the gate can be estimated from the data of Figures 15 and 22: the temperature is ~1400 K under the optimal (resonance) condition. On the other hand, the temperatures of the hot electrons and the hot phonons acquire similar values. Moreover, the temperatures are essentially higher away from the resonance. In particular, at 2DEG density of 1.4 x 10^{13} cm^{-2}, the hot-phonon lifetime is several times longer (Fig. 22, solid curve) and the hot-phonon temperature is correspondingly higher. The hot-phonon temperature is associated with enhanced lattice vibrations and may possibly contribute to device degradation through additional defect generation aggravated by the already defective GaN, aided by its pyroelectric and piezoelectric crystal structure, unless the accumulated LO-mode heat is rapidly converted into longitudinal acoustic phonons and the latter are drained away into the heat sink. Likelihood of defect generation by enhanced lattice vibrations can be further supported by strong confinement of the hot phonons to a relatively narrow portion of the momentum and real spaces in an HFET channel. It then follows that the effect of hot phonons on defect generation can be minimized at the resonant 2DEG density which causes a rapid decay of hot-phonons. This has motivated the attempts to analyze degradation of nearly lattice-matched InAlN/AlN/GaN HFETs caused by electrical stress as an indirect verification of the role of hot phonons.

8. Signature of the Resonance: HFET Phase Noise

The defect formation in stressed nearly lattice-matched InAlN/AlN/GaN HFETs is studied by the phase noise relative to the 4 GHz carrier signal on Agilent 5505 test set [46,47]. The low-

frequency phase noise technique is a very sensitive diagnostic tool for monitoring traps and offers valuable information on defect formation during stress. All stressed devices were subjected to a 7 hr DC stress at drain voltage of V_{DS}=20 V at different gate voltages corresponding to resonant and off-resonant 2DEG density conditions for the optimal decay of hot phonons. The noise is measured before and after the stress at the same conditions: V_{GS}=0V, V_{DS}=3.5V.

Figure 23 illustrates the experimental results on the spectral density of low-frequency noise measured before the stress (black curves) and after the stress (coloured lines) when the devices have been stressed at the resonance 2DEG density (9.4×10^{12} cm^{-2}) corresponding to the gate bias V_{GS}=-4V (blue line) and the off-resonance 2DEG densities corresponding to the gate bias V_{GS}=-2V (green curve) and V_{GS}=-5.5V (red curve). A dramatic increase in noise is observed at the off-resonance conditions on both sides of the resonance.

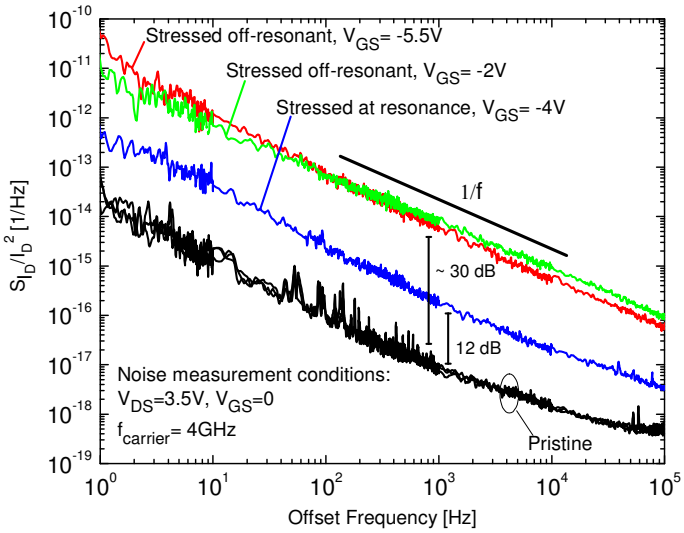

Figure 23 The normalized noise data versus the offset frequency for HFETs stressed at resonant and off-resonant 2DEG density and measured at zero gate bias [47].

The results on stress-induced defect formation are summarized in Figure 24. The stress corresponding to the resonant 2DEG density (V_{GS}=-4V) yielded a 12 dB increase in the noise power, whereas the completely off-resonant stress conditions (V_{GS}=-2V and V_{GS}=-5.5V) exhibited a dramatic increase in the noise with respect to that in the pristine devices. In particular, the noise increases by 28 dB/Hz on the left-hand side of the resonance at V_{GS}=-5.5V and by 32 dB at V_{GS}=-2V. Similar results for essentially different gate bias allow one to exclude the effect of the transverse electric field caused by the gate voltage.

The experimental data (Fig. 24, squares) are fitted with Eq. (10) (red curve), and the resonance density is estimated as 9.4×10^{12} cm^{-2}. Compared to the stress at the resonant conditions, the HFETs stressed at completely off-resonant 2DEG densities exhibit up to 16–20 dB higher noise values for the left-hand and the right-hand sides of the resonance, respectively. These results suggest that fluctuations are associated with defect generation during device degradation. At the

resonant 2DEG condition, the degradation is mild. However, under the off-resonance conditions, the noise data show up to 20 dB more noise associated with degradation of the channel and or the adjacent buffer layer.

The low-frequency noise measurements on InAlN/AlN/GaN HFETs show that the degradation due to high-field stress is 16–20 dB lower at the resonant 2DEG density of 9.4×10^{12} cm^{-2} compared with those degraded at the off-resonant conditions. The relatively small stress-induced effect on the phase noise at the resonance is attributed to the mild damage of the channel. On the other hand, at the off-resonant conditions, the additional noise is a clear evidence of dramatic generation of defects. Since the drain voltage is kept constant during all stress experiments, the damage correlates with the hot phonons rather than the electric field. The results are consistent with the phenomenon of hot-phonon build-up and the plasmon-assisted ultrafast decay of hot phonons at the resonant 2DEG density.

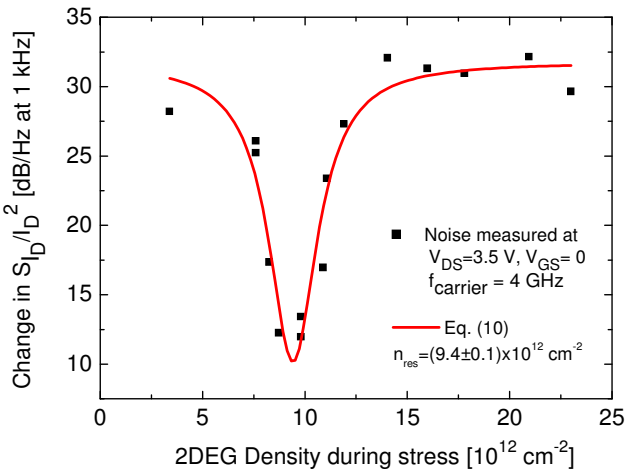

Figure 24 Increase in the noise spectral density measured at zero gate bias after 7 hr electrical stress at 20V drain bias as a function of channel 2DEG density during stress [47].

The signatures of the resonance demonstrate that the optimal HFET frequency performance (Fig. 20), the slowest HFET degradation under stress (Fig. 22), and the minimum defect formation (Fig. 24) are closely associated with the hot-phonon decay that can be approximated with Eq. (10) (Figs. 13, 15). In agreement with the resonance concept, the cut-off frequency of HFETs increases as the 2DEG density approaches the resonance value from both sides: from the low 2DEG density side and from the high 2DEG density side. In this context, the results of Fig. 1 deal with the high-density wing above the resonance. The decrease of the cut off frequency of a HFET with the increase in the 2DEG density corrrrelates with the decrease of the electron drift velocity due to the accumulation of the LO-mode heat in the channel as the hot-phonon decay becomes less efficient, because of longer hot-phonon lifetime. This correlation suggests that ultrafast dissipation of the LO-mode heat is a prerequisite for faster operation and slower degradation of nitride HFETs. These findings call for modified approaches in considering device designs for best performance and mimimum degradation.

9. Novel Camelback Channel for Improved Performance

Gallium nitride HFETs are promising power devices for microwave applications; the cut-off frequencies of short-gate HFETs exceed 200 GHz [48]. It is proverbially believed that a higher microwave power levels can be attained if the transistor channel contains more electrons. In this regard electron densities over $3x10^{13}$ cm^{-2} have been demonstrated in GaN-based heterostructures with an AlInN/AlN barrier [49]. Since the electrons are confined in the quantum well of nanometric thickness, the current density is extremely high at high electric fields, and deleterious effects due to heat accumulation come into play at high supplied power levels. The thermal conductance helps to drain out the excess acoustic phonons, but a different approach is needed to treat the LO-mode heat associated with hot optical phonons.

The hot-phonon decay is often evaluated in terms of hot-phonon lifetime (Fig. 12). It has been demonstrated that the lifetime is the shortest if the 2DEG density is in the vicinity of LO-phonon–plasmon crossover (Fig. 13). The resonance-type non-monotonous dependence on the electron density is resolved in phenomena of hot-electron transport (Figs. 19, 21), transistor cut-off frequency (Fig. 20), transistor degradation (Fig. 22) and transistor phase noise (Figs. 23, 24). For standard GaN-based channels, the resonance 2DEG density is near $6.5x10^{12}$ cm^{-2} at low electric fields, but the resonance shifts towards higher 2DEG densities as the hot-electron temperature increases (Figs. 15, 19). In voltage-biased channels, the hot electrons spread over a larger volume, and the plasma frequency decreases (Fig. 14). As a result, the resonance is observed at higher 2DEG densities, typically near $1x10^{13}$ cm^{-2} (Fig. 24).

The resonance values in typical 2DEG channels are well below the achievable 2DEG density of $3x10^{13}$ cm^{-2}, and no benefit from the LO-phonon–plasmon resonance is expected in the standard GaN-based channels at these highest 2DEG densities. The camelback channel has been proposed [39] in order to increase the 2DEG density without increasing the 3DEG density (Fig. 25). The novel camelback design combines a high 2DEG density (preferred for power operation) and ultrafast decay of hot phonons (useful for high-frequency operation and slow degradation of transistors).

The experimental study is carried out on nominally undoped $Al_{0.82}In_{0.18}N$/AlN/$Al_{0.1}Ga_{0.9}N$/GaN structures with a composite $Al_{0.1}Ga_{0.9}N$/GaN channel. Figure 25 compares the self-consistent solution of coupled Schrödinger–Poisson equations for the reference single-channel $Al_{0.82}In_{0.18}N$/AlN/GaN structure (dashed line) with the profiles obtained for the novel composite-channel structure (solid lines). The inset illustrates the band diagram of the novel structure.

The insertion of the thin $Al_{0.1}Ga_{0.9}N$ interlayer (2 nm) between the GaN and the AlN layers modifies the electron density profile, it becomes wider, and, despite of higher 2DEG density, the peak value of the 3DEG density becomes lower (Fig. 25, solid line at a 300 K). At elevated hot-electron temperatures, the 3DEG density decreases further, and the camelback profile develops (solid lines). The results on measured density profile are shown in Fig. 11 .

The hot-phonon lifetime is extracted from the hot-electron microwave noise measurements. The results for the camelback channel (Fig. 26, red bullets, [38]) are compared with those for the reference channel (open squares [10]). The lifetime decreases as the temperature increases. The

decrease has been interpreted in terms of the hot-phonon decay enhanced in the vicinity of the LO-phonon–plasmon resonance tuned by the electron heating [10].

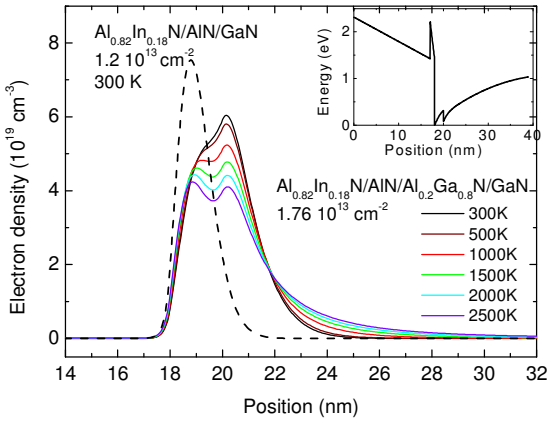

Figure 25. Calculated electron 3D density profiles for a standard structure (dashed line) and the camelback structure (solid lines) at different hot-electron temperatures [38].

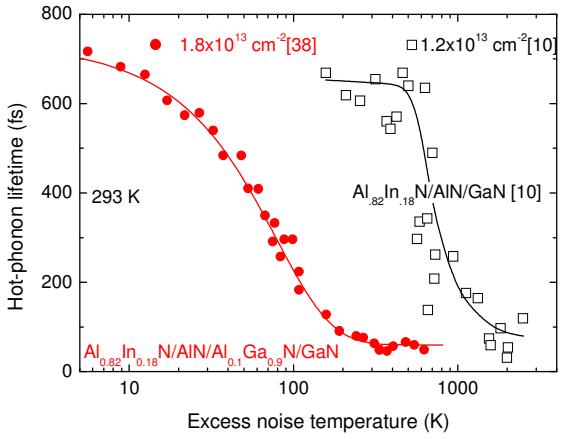

Figure 26. The hot-phonon lifetime as a function of the excess noise temperature in the reference channel (squares [10]) and the novel camelback channel (circles [38]). Curves guide the eye.

Since the equilibrium plasma frequency exceeds the LO-phonon frequency considerably in the reference channel, strong electron heating is needed to bring it into the resonance. The novel 2DEG channel contains even higher 2DEG density, 1.8×10^{13} cm^{-2} (red bullets) against 1.2×10^{13} cm^{-2} (squares) in the reference channel. Nevertheless, the camelback density profile is designed to make the plasma frequency closer to the LO-phonon frequency. As a result, the ultrafast decay of hot phonons takes place at moderate hot-electron noise temperatures (bullets) despite of high 2DEG density in the camelback channel.

10. Novel Staircase Electron Injector for Improved Efficiency

Ballistic and quasi-ballistic electron transport across the active InGaN layer, among others, are shown to be responsible for electron overflow and electroluminescence efficiency droop at high current levels in InGaN light emitting diodes (LEDs) [50–53]. In order to circumvent the hot electron transport without recombination, an electron blocking layer (EBL) can be inserted between the InGaN active layer and the p-GaN (the EBL blocks the outgoing electrons). However, the incoming holes are also blocked by the barrier in the valence band, and the EBL is not always useful. Alternatively, a novel heterostructure, a staircase electron injector (SEI), has been proposed [54], implemented, and tested [50–53]. The SEI is inserted between the n-GaN and the InGaN active region and serves for enhanced electron thermalization.

A schematic view of an $In_yGa_{1-y}N/In_zGa_{1-z}N$ staircase electron injector is shown in Fig. 27b [50]. The SEI consists of a step-like increased In composition layers and contains several conduction band discontinuities. When the electrons are injected from the n-GaN into the InGaN, they gain additional kinetic energy from the conduction band discontinuity and can bypass the active region unless they are sufficiently thermalized. The SEI enhances thermalization of the injected electrons [54].

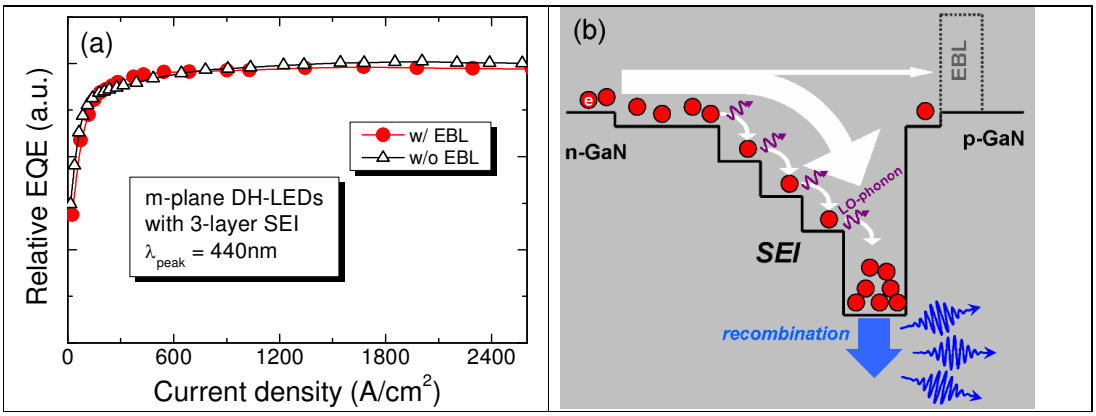

Figure 27. (a) Relative external quantum efficiency of m-plane LEDs with a 3-layer SEI and with an EBL (red bullets) and without the EBL (triangles). (b) A schematic conduction band diagram for enhanced electron thermalization [50].

Figure 27a compares the relative external quantum efficiency of the two m-plane LEDs with the same SEI [50]. The experimental data confirm that the diodes with the SEI demonstrate an essentially the same electroluminescence performance independently of the presence or absence of the EBL. An EBL is no longer needed when the SEI is used. On the other hand, if no SEI is employed, the diode without the EBL has shown substantially lower (4-5 times) electroluminescence intensity than the diode with the EBL [54]. The data of Fig. 27 support a feasible method for efficient thermalisation and elimination of parasitic ballistic and quasi-ballistic transport of the injected electrons across the active region of InGaN light emitting diodes.

11. Main Results and Conclusions

The experimental investigation of fluctuations is a source of information on fast and ultrafast processes responsible for HFET performance and damage. A novel fluctuation-based approach, based on hot-electron velocity fluctuations measured at a microwave frequency, is used for prediction of nitride HFET operation and failure. The following statements summarize the main results:

1. The resonance-type dependence of hot-phonon lifetime on 2DEG density is resolved from the electron velocity fluctuations.
2. The optimal density for ultrafast dissipation of the LO-mode heat is estimated for the 2DEG channels located in GaN and InGaAs.
3. The optimal 2DEG density depends on the supplied power.
4. The HFET degradation is slower and the operation is faster when the LO-mode heat is dissipated faster.
5. The signatures of plasmons are found in electron velocity fluctuations, hot-phonon lifetime, electron drift velocity, HFET cutoff frequency, HFET phase noise, and HFET damage.
6. The novel heterostructre is proposed, implemented, and tested for improved ultrafast decay of LO-mode heat.
7. The novel heterostructre is proposed, implemented, and tested for improved efficiency of light emitting diodes.
8. The fluctuation-based approach is proposed for improved device performance and mitigated device damage.

References

[1] H. Morkoç, *Handbook of Nitride Semiconductors and Devices*, Vol. 3 (Wiley-VCH, Weinheim, 2009).

[2] M.S. Shur, R. Gaska, "Deep-ultravioled light-emitting diodes", *IEEE Transactions on Electron Devices* **57** 12–25 (2010).

[3] F. Medjdoub, J.-F. Carlin, C. Gaquiere, N. Grandjean, and E. Kohn, "Status of the emerging InAlN/GaN power HEMT technology," *The Open Electrical and Electronic Engineering Journal* **2** 1–7, (2008).

[4] M. Higashiwaki, T. Mimura, and T. Matsui, "Development of high-frequency GaN HFETs for millimeter-wave applications," *IEICE Transactions on Electronics* **E91-C** 984–988, (2008).

[5] M. Higashiwaki, T. Mimura, and T. Matsui, "AlGaN/GaN heterostructure field-effect transistors on 4H-SiC substrates with current-gain cut-off frequency of 190 GHz," *Applied Physics Express* **1** 021103, (2008).

[6] A. Matulionis, J. Liberis, I. Matulionienė, M. Ramonas, E. Šermukšnis, J.H. Leach, M. Wu, X. Ni, X. Li, and H. Morkoç, "Plasmon-enhanced heat dissipation in GaN-based two-dimensional channels," *Applied Physics Letters* **95** 192102/1–3 (2009).

[7] J.H. Leach, C.Y. Zhu, M. Wu, X. Ni, X. Li, J. Xie, Ü. Özgür, H. Morkoç, J. Liberis, E. Šermukšnis, A. Matulionis, T. Paskova, E. Preble, and K.R. Evans, "Effect of hot phonon lifetime on electron velocity in InAlN/AlN/GaN heterostructure field effect transistors on bulk GaN substrates," *Applied Physics Letters.* **96** 133505/1–3 (2010).

[8] J.H. Leach, M. Wu, X. Ni, J. Lee, Ü. Özgür, H. Morkoç, J. Liberis, E. Šermukšnis, A. Matulionis, H. Cheng, and Ç. Kurdak, "Degradation in InAlN/GaN-based heterostructure field effect transistors: Role of hot phonons," *Applied Physics Letters* **95** 223504/1–3 (2009).

[9] B. K. Ridley, "The LO phonon lifetime in GaN," *Journal of Physics: Condensed Matter* **8**, L511–L513, (1996).

[10] A. Matulionis, J. Liberis, I. Matulionienė, M. Ramonas, and E. Šermukšnis, "Ultrafast removal of LO-mode heat from a GaN-based two-dimensional channel," *Proceedings of IEEE* **98** 1118–1126 (2010).

[11] A. Matulionis, "Ultrafast decay of non-equilibrium (hot) phonons in GaN-based 2DEGchannels," *Physica Status Solidi(C) Conferences* **6** (12) 2834–2839, (2009).

[12] A. Matulionis, J. Liberis, and H. Morkoç, „Plasmon-assisted dissipation of LO-mode heat in nitride 2DEG channels",*Proceedings of* SPIE **7602** 76020H/1–6, (2010).

[13] A. Dyson and B.K. Ridley, "Phonon–plasmon coupled-mode lifetime in semiconductors," *Journal of Appllied. Physics* **103** 114507, (2008).

[14] A. Matulionis, J. Liberis, E. Šermukšnis, J. Xie, J.H. Leach, M. Wu, and H. Morkoç, *Semiconductor Science and Technology* **23** 075048/1−6 (2008).

[15] G. Xu, S. Tripathy, X. Mu, Y. Ding, K. Wang, Y. Cao, D. Jena, and J. Khurgin, "Stokes and anti-Stokes Raman scatterings from biased GaN/AlN heterostructure," *Applied Physics Letters* **93** 051912 (2008).

[16] A. Matulionis, J. Liberis, I. Matulionienė, M. Ramonas, L.F. Eastman, J.R. Shealy, V. Tilak, and A. Vertiatchikh, "Hot-phonon temperature and lifetime in a biased $Al_xGa_{1-x}N$/GaN channel estimated from noise analysis," *Physical Review* **B 68** 035338/1-7 (2003).

[17] L. Ardaravičius, M. Ramonas, J. Liberis, O. Kiprijanovič, A. Matulionis, J. Xie, M. Wu, J. H. Leach, H. Morkoç, "Electron drift velocity in lattice matched AlInN/AlN/GaN channel at high electric field", *Journal of Applied Physics* **106** 073708/1–5 (2009).

[18] H. L. Hartnagel, R. Katilius, and A. Matulionis, *Microwave Noise in Semiconductor Devices* (Wiley, New York, 2001).

[19] A. Matulionis and I. Matulionienė, "Hot-electron noise in III-V semiconductor structures for ultra-fast devices"in: *Noise and Fluctuations Control in Electronic Devices*, edited by A. A. Balandin (American Scientific Publishers, Stevenson Ranch, 2002), pp. 249−266.

[20]A. Matulionis, "Hot phonons in GaN channels for HEMTs"*Physica Status Solidi(A) Applications and Materials* **203**(10) 2313–2325 (2006).

[21] A. Matulionis, I. Matulionienė, "Accumulation of hot phonons in GaN and related structures (invited)" *Proceedings of SPIE* **6473** 64730P/1−15 (2007).

[22] A. Matulionis, "GaN-based two-dimensional channels: hot-electron fluctuations and dissipation (invited)", *Journal of Physics: Condensed Matter* **21** 174203/1–8 (2009).

[23] J. Liberis, I. Matulionienė, A. Matulionis, E. Šermukšnis, J. Xie, J. H. Leach, and H. Morkoç, "InAlN-barrier HFETs with GaN and InGaN channels", *Physica Status Solidi(A) Applications and Materials,* **206** (7) 1385–1395 (2009).

[24] V Aninkevičius, A Matulionis, I. Matulionienė, "Hot-phonon lifetime in a modulation-doped AlInAs/GaInAs/AlInAs/InP", *Semiconductor Science and Technology* **20** (2), 109–114 (2005).

[25] J. Liberis, I. Matulionienė, A. Matulionis, M. Lemme, H. Kurz, M. Först, "Hot-phonon temperature and lifetime in biased boron-implanted SiO_2/Si/SiO_2 channels", *Semiconductor Science and Technology* **21**, 803–807 (2006).

[26] A Matulionis, J. Liberis, I. Matulionienė, H.-Y. Cha, L. F. Eastman, M. G. Spencer, "Hot-Phonon temperature and lifetime in biased 4H-SiC", *Journal of Applied Physics* **96** (11), 6439–6444 (2004).

[27] J. Liberis, I. Matulionienė, A. Matulionis, M. Ramonas, L. F. Eastman, „Hot phonons in high-power microwave HEMT and FET channels", in *„Advanced semiconductor materials and devices research - SiC and III-Nitrides",* Ho-Young Cha, ed. (Transworld Research Network, Kerala, India, 2009), pp. 203–257.

[28] A. Matulionis and H. Morkoç, „Hot phonons in InN-contained heterostructure 2DEG channels (invited)", *Proceedings of SPIE* **7216,** 721608/1–14 (2009).

[29] J.H. Leach, X. Ni, Ü. Özgür, A. Matulionis, and H. Morkoç „New twists in LEDs and HFETs based on III-V nitride semiconductors (feature article)" *Physica Status Solidi(A) Applications and Materials* **207** (5) 1091-1100 (2010).

[30] M. Ramonas, A. Matulionis, J. Liberis, L.F. Eastman, X. Chen, and Y.-J. Sun, "Hot-phonon effect on power dissipation in a biased AlGaN/AlN/GaN channel" *Physical Review* **B 71** 075324/1−8 (2005).

[31] M. Ramonas and A. Matulionis, "Monte Carlo simulation of hot-phonon effects in biased nitride channels "in: *New Research in Semiconductors,* edited by T.B. Elliot (Nova Science Publishers Inc., Hauppauge, NY, USA, 2006) pp. 95–121.

[32] A. Matulionis, J. Liberis, and M. Ramonas, **"**Microwave noise in biased AlGaN/GaN and AlGaN/AlN/GaN channels" *American Institute of Physics Conference Proceedings* **CP780** 105–108 (2005)

[33] X.L. Lei and N.J.M. Horing, "Thermal noise temperature of GaAs heterosystems for steady-state hot-electron transport with nonequilibrium phonons," *Physical Review* **B 36** 4238–4248 (1987).

[34] A. Matulionis, J. Liberis, M. Ramonas, I. Matulionienė, L.F. Eastman, A. Vertiatchikh, X. Chen, and Y.J. Sun, "Hot-electron microwave noise and power dissipation in AlGaN/AlN/GaN channels for HEMTs" *Physica Status Solidi(C) Conferences* **2** (7) 2585–2588 (2005).

[35] Z. Wang, K. Reimann, M. Woerner, T. Elsaesser, D. Hofstetter, J. Hwang, W.J. Schaff, and L.F. Eastman, "Optical phonon sidebands of electronic intersubband absorption in strongly polar semiconductor heterostructures," *Physical Review Leters* **94** 037403, (2005).

[36] J.A. Kash and J.C. Tsang, "Nonequilibrium phonons in semiconductors" in: Spectroscopy of Nonequilibrium Electrons and Phonons, edited by C.V. Shank, and B.P. Zakharchenya, *Modern Problems in Condensed Matter*, Vol. 35 (Elsevier, Amsterdam, North Holland, 1992), pp. 113−167.

[37] K.T. Tsen, J.G. Kiang, D.K. Ferry, and H. Morkoç, "Subpicosecond time-resolved Raman studies of LO phonons in GaN: dependence on injected carrier density," *Applied Physics Letters* **89** 112111, (2006).

[39] E. Šermukšnis, J. Liberis, M. Ramonas A. Matulionis, J.H. Leach, M. Wu, V. Avrutin, and H. Morkoç „Camelback channel for fast decay of LO phonons in GaN heterostructure field-effect transistor at high electron density", *Applied Physics Letters* **99** 043501 (2011)

[39] J. H. Leach, M. Wu, H. Morkoç, M. Ramonas, and A. Matulionis. „Heterostructure designs for enhanced performance and reliability in GaN HFETs: Camelback channels" *Proceedings of SPIE* **7939** 79391P-1-10 (2011).

[40] A. Matulionis, J. Liberis, I. Matulionienė, E. Šermukšnis, J. H. Leach, H. Morkoç, „Optimal conditions for heat dissipation in nitride HFETs: power tunable plasmon-LO-phonon resonance (invited)", *Abstracts and program of Workshop on Compound Semiconductor Devices and Integrated Circuits* (WOCSDICE 2010), May 17-19, 2010 Darmstadt/Seeheim, Germany, pp. 191-194.

[41] A.Matulionis, J. Liberis, I. Matulionienė, E. Šermukšnis, J.H. Leach, M. Wu, H. Morkoç, "Novel fluctuation-based approach to optimization frequency performance and degradation of nitride heterostructure field effect transistors" (invited), *Physica Status Solidi(A) Applications and Materials* **208** (1) 30-36 (2011).

[42] E.Šermukšnis, J. Liberis, A. Matulionis, **"**Microwave noise technique for measurement of hot-electron energy relaxation time and hot-phonon lifetime", *Lithuanian Journal of Physics* **47** (4), 491–498 (2007).

[43] L.Ardaravičius, J. Liberis, *Lithuanian Journal of Physics*, **40** 357 (2000).

[44] L. Ardaravičius, J. Liberis, O. Kiprijanovič, A. Matulionis, M. Wu, and H. Morkoç. "Hot-electron drift velocity and hot-phonon decay in AlInN/AlN/GaN" *Physica Status Solidi Rapid Research Letters* **5**(2–3) 65–67 (2011).

[45] N. Moll, M.R. Hueschen, and A. Fischer-Colbrie, *IEEE Transactions on Eelectron Devices* **35** (7) 879-886 (1988).

[46] C. Kayis, J. H. Leach, C. Y. Zhu, Mo Wu, X. Li, Ü. Özgür, H. Morkoç, X. Yang, V. Misra, P. H. Handel, *IEEE Electron Device Letters*, **31**, 1041 (2010).

[47] C. Kayis, R. A. Ferreyra, M. Wu, X. Li, Ü. Özgür, A. Matulionis, H. Morkoç. „Degradation in InAlN/AlN/GaN heterostructure field-effect transistors as monitored by low-frequency noise measurements: Hot phonon effects", *Applied Physics Letters* **99** 063505 (2011).

[48] H. Sun, A. R. Alt, H. Benedickter, E. Feltin, J-F. Carlin, M. Gonschorek, N. Grandjean, and C. R. Bolognesi, *Physica Status Solidi(A) Applications and Materials* **208** 429 (2011).

[49] M. Gonschorek, J.-F. Carlin, E. Feltin, M. A. Py, N. Grandjean, V. Darakchieva, B. Monemar, M. Lorenz, and G. Ramm, *Journal of Applied Physics* **103** 093714 (2008).

[50] Ü. Özgür, X. Ni, X. Li, J. Lee, S. Liu, S. Okur, V. Avrutin, A. Matulionis**,** and H. Morkoç, "Ballistic transport in InGaN-based LEDs: impact on efficiency (invited)", *Semiconductor Science and Technology* **269** 014022/1-12 (2011).

[51] X. Ni, X. Li, J. Lee, S. Liu, V. Avrutin, A. Matulionis, Ü. Özgür, and H. Morkoç, "Pivotal role of ballistic and quasi-ballistic electrons on LED efficiency (review)", *Superlattices and Microstructures* **48**(2) 133–153 (2010).

[52] J. H. Leach, X. Ni, J. Lee, Ü. Özgür, A. Matulionis, H. Morkoç, „New twists in LEDs and HFETs based on nitride semiconductors (invited)"**,** *Physica Status Solidi (A) Applications and Materials* **207**(5) 1091–1100 (2010).

[53] X. Ni, X. Li, J. Lee, S. Liu, V. Avrutin, Ü. Özgür, H. Morkoç, A. Matulionis, T. Paskova, G. Mulholland, and K.R. Evans, "The effect of ballistic and quasi-ballistic electrons on the efficiency droop of InGaN light emitting diodes," *Physica Status Solidi Rapid Research Letters* **4**(8–9) 194–196 (2010).

[54] X. Ni, X. Li, J. Lee, S. Liu, V. Avrutin, Ü. Özgür, H. Morkoç, A. Matulionis, T. Paskova, G. Mulholland, and K.R. Evans, „InGaN staircase electron injector for reduced electron overflow in InGaN light emitting diodes," *Applied Physics Letters* **97**(3) 031110-1–3 (2010).

List of Symbols, Abbreviations, and Acronyms

HFET – hetereostructure field effect transistor
2DEG – two-dimensional electron gas
2DEG density – electron sheet density
3DEG – three-dimensional electron gas
3DEG density – electron density per unit volume
SEI – staircase electron injector
EBL – electron blocking layer
LED – light emitting diode
RF – radio frequency
X-band – microwave frequency band near 10 GHz
cut-off frequency – unity gain frequency
millimeter-wave frequencies – above30 GHz, below 300 GHz
X-ray diffraction – diffraction of Roentgen rays
JCA812 – microwave low noise amplifier
SR250 – gated integrator and boxcar averager module (Stanford Research Systems)
SR240A – quad fast amplifier (Stanford Research Systems)
SR245 – computer interface module (Stanford Research Systems)
RS232 – interface module
Labview – computer software
PC – personal computer
OMVPE – organo-metallic vapor phase epitaxy
heterojunction – monocrystallic interface of two semiconductors with different bandgap
heterostructure – monocrystallic structure that contains one or more heterojunctions
LA phonons – longitudinal acoustic phonons
LO phonons – longitudinal optical phonons
TO phonons – transverse optical phonons
LO-mode heat – heat accumulated by non-equilibrium LO phonons
hot electrons – non-equilibrium high energy electrons
hot phonons – LO phonons launched by hot electrons
hot-phonon lifetime – time constant for conversion of hot phonons into migrant modes
plasmons – quanta of collective vibrations of electrons
plasmon–LO-phonon crossover – plasmon energy equals LO-phonon energy
thermal walkout – time-dependent variation of measurables caused by device self-heating
ultrafast – in subpicosecond range
a, b, and c are the coefficients in Eq. (10)
f is the frequency
$f(\varepsilon)$ is the electron-temperature-dependent Fermi–Dirac electron distribution function
$\hbar\omega_{LO}$ is the LO-phonon energy
I is the current
k_B is the Boltzmann constant
n_{2D} is the 2DEG density
N_{el} is the number of electrons in the channel
N_{LO} is the hot-phonon mode occupancy
n_{cr} is the plasmon–LO-phonon crossover electron density

n_{res} is the resonance 2DEG density
$p^{\pm}$ are the probabilities to find a suitable electron
$\Delta P_n(f)$ is the available noise power
P_d is the dissipated power per electron
P_s is the supplied electric power per electron
$T_n(f)$ is the hot-electron noise temperature
T_e is the hot-electron temperature
T_{LO} is the hot-phonon temperature
τ_{LO} is the hot-phonon lifetime
τ_{sp} is the mean time for spontaneous emission of an LO-phonon by a hot electron
τ_{abs} is the mean time for LO-phonon absorption by any of the electrons
τ_ε is the hot-electron energy (temperature) relaxation time
U is the applied voltage
V_{GS} is the gate–source voltage
V_{DS} is the drain–source voltage.